sustainability

MDPI

Article

Firefly Algorithm-Based Photovoltaic Array Reconfiguration for Maximum Power Extraction during Mismatch Conditions

Mohammad Nor Rafiq Nazeri [1], Mohammad Faridun Naim Tajuddin [1], Thanikanti Sudhakar Babu [2,*], Azralmukmin Azmi [1], Maria Malvoni [3,*] and Nallapaneni Manoj Kumar [4,*]

1 Faculty of Electrical Engineering Technology, Universiti Malaysia Perlis, Kangar 01000, Malaysia; rafiqnazeri93@gmail.com (M.N.R.N.); faridun@unimap.edu.my (M.F.N.T.); azralmukmin@unimap.edu.my (A.A.)
2 Department of Electrical and Electronics Engineering, Chaitanya Bharathi Institute of Technology, Gandipet, Hyderabad 500075, India
3 School of Electrical and Computer Engineering, National Technical University of Athens, 15780 Athens, Greece
4 School of Energy and Environment, City University of Hong Kong, Kowloon, Hong Kong
* Correspondence: sudhakarbabu66@gmail.com (T.S.B.); maria.malvoni@gmail.com (M.M.); mnallapan2-c@my.cityu.edu.hk (N.M.K.)

Abstract: This studyaimed at improving the performance and efficiency of conventional static photovoltaic (PV) systems by introducing a metaheuristic algorithm-based approach that involves reconfiguring electrical wiring using switches under different shading profiles. Themetaheuristicalgorithmused wasthe firefly algorithm (FA), which controls the switching patterns under non-homogenous shading profiles and tracks the highest global peak of power produced by the numerous switching patterns. This study aimed to solve the current problems faced by static PV systems, such as unequal dispersion of shading affecting solar panels, multiple peaks, and hot spot phenomena, which can contribute to significant power loss and efficiency reduction. The experimental setup focusedon software development and the system or model developed in the MATLAB Simulink platform. Athorough and comprehensive analysis was done by comparing the proposed method's overall performance and power generation with thenovel static PVseries–parallel (SP) topology and totalcross-tied (TCT) scheme. The SP configuration is widely used in the PV industry. However, the TCT configuration has superior performance and energy yield generation compared to other static PV configurations, such as the bridge-linked (BL) and honey comb (HC) configurations. The results presented in this paper provide valuable information about the proposed method's features with regard toenhancing the overall performance and efficiency of PV arrays.

Keywords: photovoltaic cells; mismatch losses; partial shading; firefly; maximum power extraction

check for updates

Citation: Nazeri, M.N.R.; Tajuddin, M.F.N.; Babu, T.S.; Azmi, A.; Malvoni, M.; Kumar, N.M. Firefly Algorithm-Based Photovoltaic Array Reconfiguration for Maximum Power Extraction during Mismatch Conditions. *Sustainability* **2021**, *13*, 3206. https://doi.org/10.3390/su13063206

Academic Editor: Tamer Khatib

Received: 29 December 2020
Accepted: 8 March 2021
Published: 15 March 2021

1. Introduction

Solar energy is currently a demanding renewable power source forenergy supply. Solar energy hasan infinite supply, a simple installation process in remote areas [1], and is eco-friendly in nature. The solar module takes insolar energy or lightandgenerates electricity by absorbing the photon energy obtained from the sunlight and causing apotential difference, which allows the movement of electrons between the p–n junctions in the solar module. This process is called the photovoltaic effect. Therefore, the nonlinearity of the global maximum power peak (G_{MPP}) and solar photovoltaic (PV) performance depends on the surrounding factors, such as atmospheric temperature, solar irradiation, and partial shading conditions [2,3]. To represent the effect of irradiation, different levels of irradiation and theirrespective power curves areplotted in Figure 1. Due to varying levels of irradiation falling on PV modules, partial shading exists. This partial shading causes multiple peaks in power-voltage (P–V) curves and the presence of different current levels in the PV array.

The occurrence of different levels of irradiationproduces multiple peaks in P–V curves, as can be observed in Figure 2.

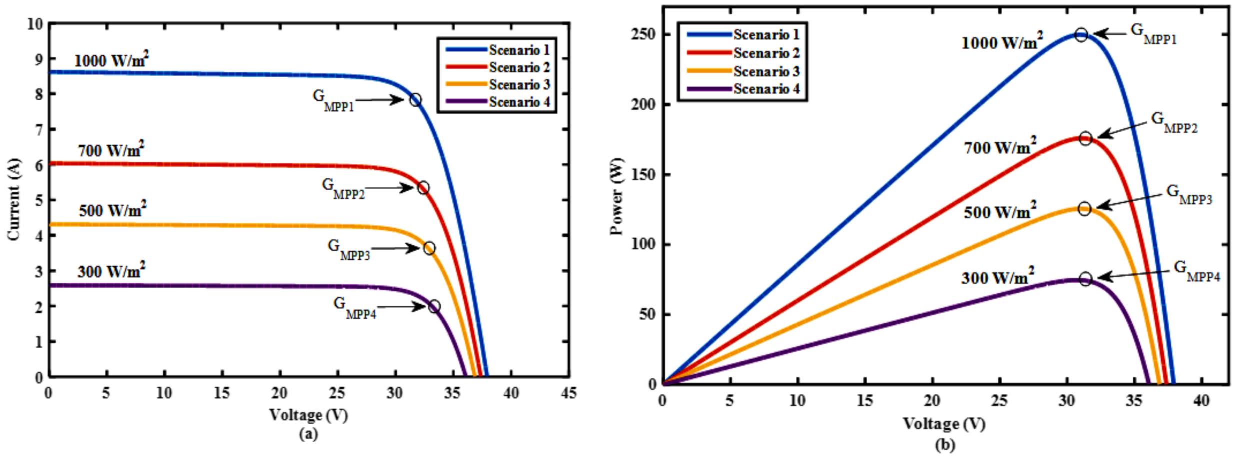

Figure 1. The effect of different irradiaton levels on the global maximum power peak (G_{MPP}) (**a**) Current–Voltage I–V and (**b**) Power–Votlage P–V curves.

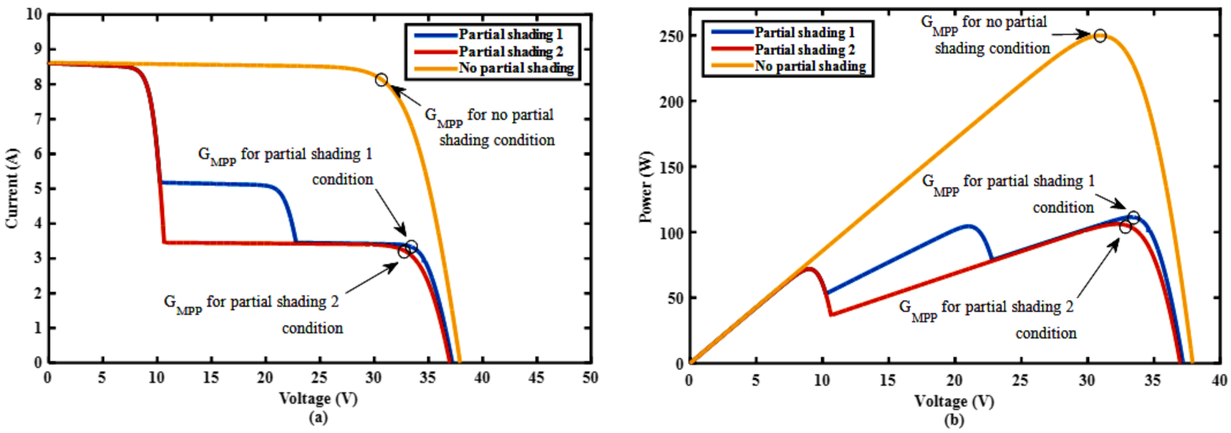

Figure 2. The multiple peaks effects of the G_{MPP} (**a**) I–V and (**b**) P–V curves due to the partial shading states.

Even though solar energy possesses various benefits, it has low conversion efficiency [4] and theinitial capital required and installation costs are expensive. These have become a limitation or barrier tothe PV system becoming one of the leading solutionsforsustainable power generation [5]. Hence, to fully utilize the PV application as the main source of power generation, previous research has introduced numerous solutions to increase the efficiency ofPVsystems in excellent conditions and thus enablePV systemsto meet future energy needs [6,7].

One of the methods that has been introduced to maximize efficiency, and extract as much power as possible, is by utilizing an algorithm to track the maximum power point (MPP) [8]. The power feedback method is a common maximum power point tracking (MPPT) topology that has been widely used as a measurement of the array power and feedback variable. Three typical MPPT tracking methods are based on power feedback applications.Commonly embraced algorithms for PV power systems are the perturb and observe (P&O) method [9,10], the incremental conductance (IncCond) method [11], and the hill climbing (HC) method [12]. Flow charts of the HC and P&O/IncCond methods can be seen in Figure 3a,b, respectively.

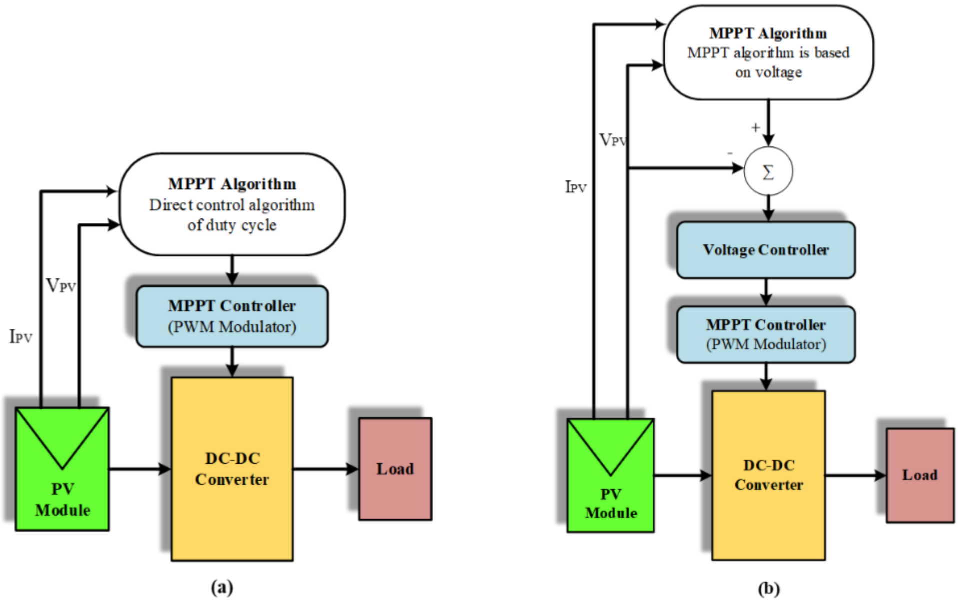

Figure 3. Typical block diagrams for the (**a**) hill climbing (HC) method and (**b**) perturb andobserve (P&O) and incremental conductance (IncCond) methods in photovoltaic (PV) applications.

Both the IncCond and P&O methods modulate the solar array voltage to trace an optimal set point. In contrast, the MPPT-based HC method presents a perturbation in the power converter's duty cycle. Even though the conventional MPPT tracking methods are simple, their performance under rapid, inconsistent climate changes is highly compromised. The basic algorithm cannot efficiently track the MPP, particularly underpartially shaded PV array conditions [13].

Also, various static interconnection schemes have been introduced to form PV arrays, such as the (a) series–parallel (SP), (b) bridge-linked (BL), (c) honey comb (HC), and (d) total cross-tied (TCT) methods, in order to overcome the mismatch power losses and increase PV array power during partial shading circumstances [14]. The connection diagrams for theSP, BL, HC, and TCT methods are shown in Figure 4a–d, respectively.

According to previous studies [15,16], the TCT scheme shows energetic performances and a higher fill factor [17], and is the most commonly used interconnection scheme for power enhancement during multiple peaks conditions, with a considerablly high-efficiency reduction of mismatch power losses. However, the SP interconnection is more commonly used in practice in PV system application power plantsthanthe TCT topology [18]. The electrical connections of the TCT and SuDoKu methods are shown in Figure 5.

Researchers have recently established a new approach to overcome the effect of partial shading in PV systemsby usingPV array reconfiguration methods [19].This approach involves evolutionary computation (EC) algorithms, such as particle swarm optimization (PSO), the genetic algorithm (GA), ant colony optimization (ACO), and differential evolution (DE) [19–21]. Other than these, the zig-zag and SuDoKu methods [22,23] have also been introduced to overcome this issue.The various array reconfiguration methods that are practically used can be categorized into (1) relocation of physical PV panels [23], (2) electrical PV system rewiring [24], and (3) reconfiguration of the electrical array [25–27].

The earlier method requiresa complex electrical wiring scheme, highly skilled labor, and complicated electrical switching to solve the partial shading drawbacks of the PV array [19]. Therefore, the PV application's optimization technique is envisaged as the most suitable solution to address the drawbacks mentioned above. This technique enableda superior performance in handling multimodal objective functions and switching combination identification for PV array reconfiguration. A comprehensive technical evaluation of aPV array reconfiguration optimization technique based on firefly algorithm (FA) is proposedin this paper, in orderto overcome the rapidly changingirradiation conditions and the partial shading circumstances. The reconfiguration method presented in this paper is based on the SP topology.This topology is selectedbecause it is a commonly employed PV array configuration. Its electrical wiring is less complicated, involves low capital and installation costs, and requires fewer switches thanthe reconfiguration methods implemented in TCT and other complex architectures [23,26].

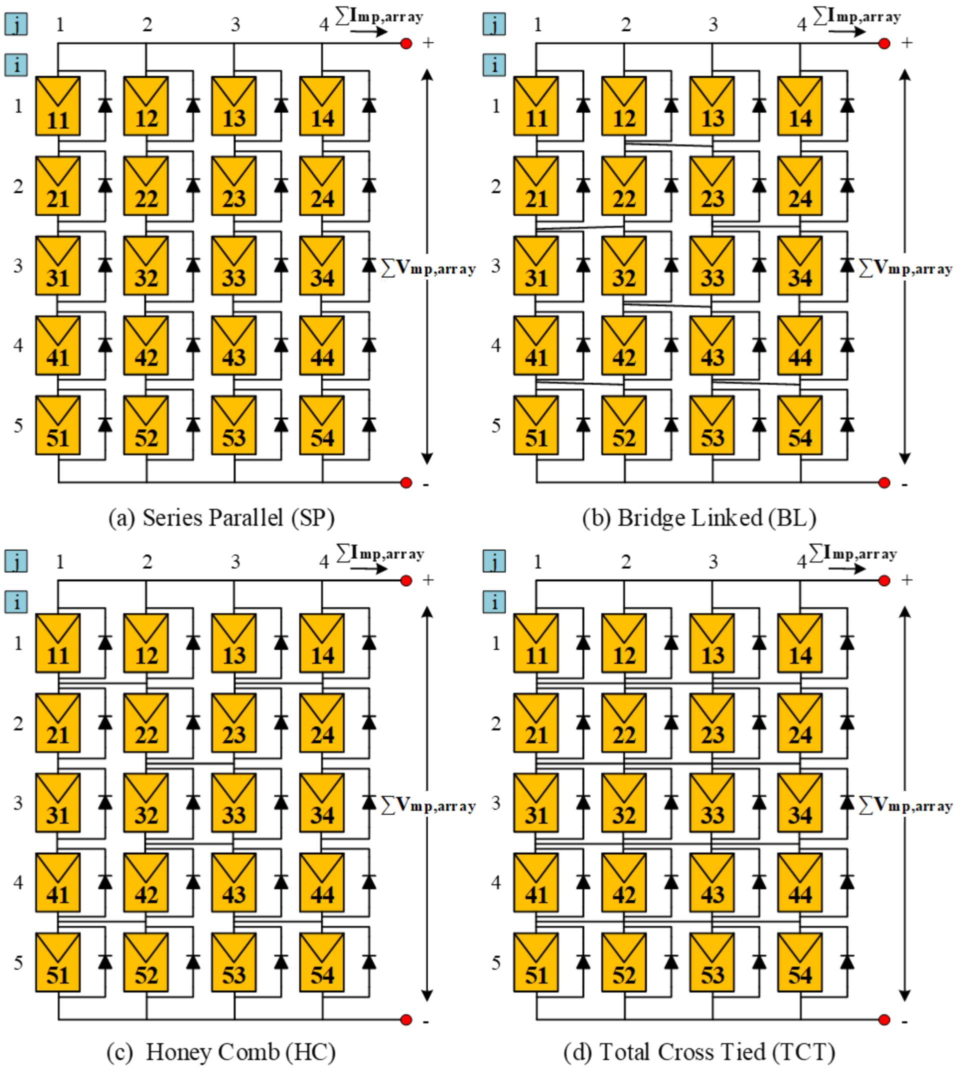

Figure 4. Different interconnection schemes for 5 × 4 PV array size configurations: (**a**) series–parallel, (**b**) bridge–linked, (**c**) honey comb, (**d**) total cross-tied.

The non-linearity of the P–V and I–V characteristic curves ofPV systems varies depending on the temperature of the environment and the irradiance given offby the sun [15,24]. The uncertainty of the surrounding climate will affect the MPP of the PV system, and multiple peaks might occur given theuncertainty of the exposure ofthe solar modules to solar irradiation in a series string. The changes in the values ofthe irradiance absorbed by the solar arrays will cause the G_{MPP} to converge away from the load's optimal operating power. Figure 6a,b show the effects of shading circumstances onthe divergence of the intersection between the PV array G_{MPP} and the load.

Based on Kirchhoff's voltage law, the PV cells that are partially shaded will contribute to the negative voltage and become loads of the circuit. The shaded PV module also consumes the power generated by the other non-shaded PV cells in the form of heat, leading to the destruction of the PV module. Even worse, it can demolish the photovoltaic cells' internal structure, and lead to a kind of permanent damage called the "hot spot" phenomenon.

This effect is due to the long-term and continuous exposure to high-temperature heat accumulation [28,29]. The majority of industrialcorporations involved in solar cell commercial products use a bypass diode connected in parallel with the PV array in order to overcome the hot spot phenomenon. This method can undeniably extend the lifespan of the solar modules. However, another tradeoff might occur, such as greater power losses and energy reduction, since the bypass diodes also consume energy when the current passes through them [26].Therefore, the reconfiguration of the mode of thePV modules' interconnection in the array seems effective in preventing the reduction in PV output power [30,31].

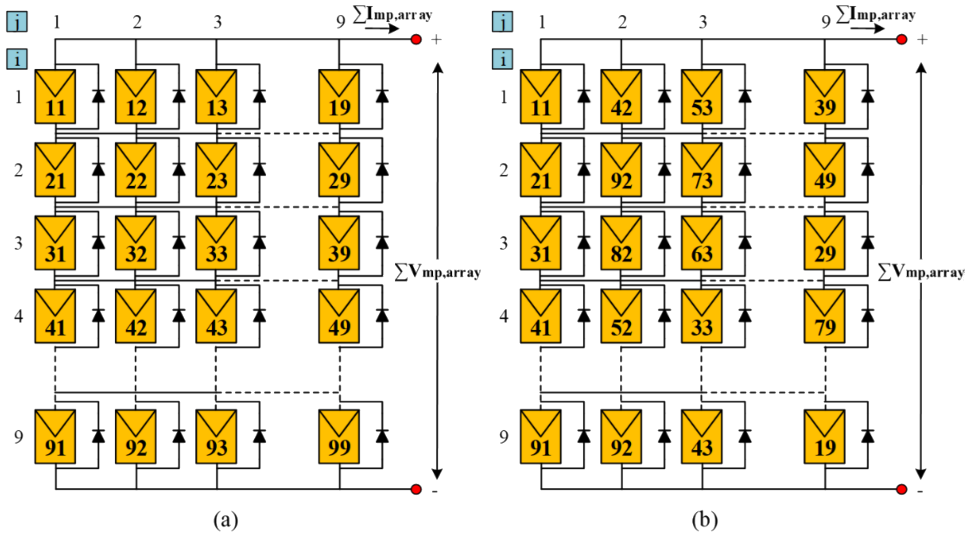

Figure 5. Example of PV array reconfiguration: (**a**) 9 × 9 array size of the TCT topology and (**b**) reconfiguration of PV array physical location with the SuDoKu method.

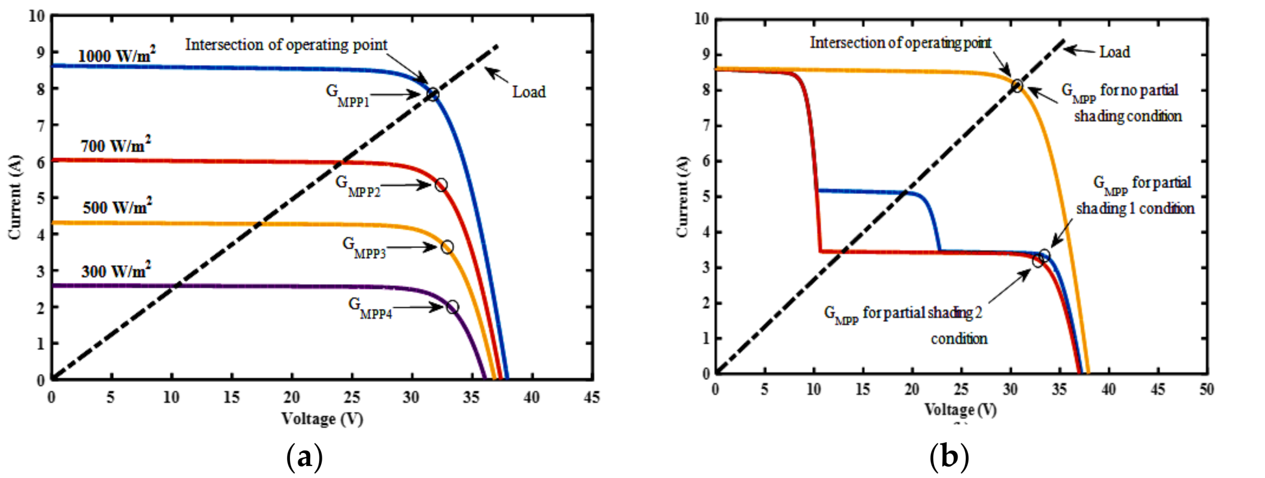

Figure 6. The intersection of the operating point between G_{MPP} and the load under numerous shading conditions; (**a**) symmetry shading pattern, and (**b**) unsymmetrical partial shading (PS) pattern.

Past Studies Related to the Reconfiguration Technique in the PV Array System

Much researchhas been carried outto improvePV systems' usage by maximizing the PV array's efficiency. The researchers aim to maximize the power derived from the solar arrays as much as possible, and reduce the energy wastage due to shading effects. Table 1 summarizes the methods undertakenby previous researchers usingthe reconfiguration of electrical array (REA) method.

Table 1. Review of past studies related to the reconfiguration of electrical array (REA) method in solar system application.

Ref	Type of Interconnection and Array Size	Control Algorithm/Technique	Remarks
[19]	Total Cross Tied (TCT) 9 × 9 array size	Particle swarm optimization (PSO)	Relocation of physical PV arrays based on particle swarm optimization (PSO) is proposed in this paper. Extensive simulations were done for the proposed method, which involves the electrical connections' alteration while the physical location remains static.
[17]	Total Cross Tied (TCT) 9 × 9 array size	Standard deviation genetic algorithm (SDGA)	The method introduced in this paper involved the standard deviation genetic algorithm (SDGA) as an optimization algorithm for electrical connection adjustment, while the PV array's physical location remains unchanged. As a result of the final connection matrix, uniform shade dispersion throughout the panels with new electrical interconnection was obtained to boost the PV array's maximum power.
[16]	Total Cross Tied (TCT) 9 × 9 array size	Genetic algorithm (GA)	The genetic algorithm (GA) technique was implemented in this paper for the total cross tied (TCT) scheme to establish a new electrical configuration and enhance the PV arrays' output power. The method modified the electrical connections, and the physical location of the solar panel was fixed.
[32]	Total Cross Tied (TCT) 3 × 3 array size	Scanning algorithm (SA) with adaptive part and fixed part scheme	A novel algorithm entitled configuration scanning algorithm (SA) had been executed in this paper to verify all possible electrical connections by utilizing the solar panel's short current values measured at particular parts only. Each row of an array is arranged by connecting the panels with the closest short circuit current values.
[33]	Total Cross Tied (TCT) 9 × 9 array size	Sudoku	This paper implemented a fixed reconfiguration solution based on the Sudoku puzzle pattern as an optimization tool to minimize the shading effects. The PV array's physical location in a total cross tied (TCT) scheme had been rearranged based on a new modification of Sudoku dispersion rules.
[34]	Total Cross Tied (TCT) 4 × 3 array size	Particle swarm optimization (PSO) with fixed part and adaptive switching controls	This paper proposed an adaptive reconfiguration solution for module arrays to maximize the PV generation output power. The strategy used is based on the particle swarm optimization (PSO) algorithm to detect if shading or malfunctions of the PV array have occurred; after that, the algorithm immediately reconfigures the optimal PV array connection.
[22]	Total Cross Tied (TCT) 9 × 9 array size	Sudoku	This paper's reconfiguration method is based on the Sudoku puzzle pattern, using it in distributing shading effects throughout the PV arrays without reconfiguring the electrical connections in a total cross tied (TCT) scheme.
[35]	Total Cross Tied (TCT) 3 × 3 array size	Bubble sort of modelbase with an adaptive bank and fixed part	This paper implemented an adaptive reconfiguration scheme for the reduction of shading's negative effects. A switching matrix controller connects the adaptive solar bank and a fixed part of the PV module arrays to increase the output power production in real-time.
[36]	Total Cross Tied (TCT) 4 × 4 array size	Irradiance equalization	A dynamic reconfiguration algorithm based on the irradiance equalization principle wasemployed in this paper to mitigate the spatial uncertainty irradiance causing negative effects on the PV array's power production. The authorshave aimed to create balanced irradiance dispersion in a row of interconnected series of PV arrays, and utilize the irradiance threshold to achieve the nearest optimal configuration ofirradiance equalization.
[37]	Series-Parallel (SP) 3 × 2 array size	Electrical array reconfiguration (EAR) with static part and dynamic part	The authors applied dynamical electrical array reconfiguration (EAR) to raise the energy production of a grid-connected PV system under numerous operating conditions. The strategy is appliedusing a controllable switching matrix between the central inverter and the PV generator.

Most previous researchers, such as [19,36], implemented the REA method inthe TCT scheme as an alternative solution in dealing with theshading effects. The TCT topology undeniably provides superior and more energetic performances by generating the most power production under various shading patterns and mismatching conditions, compared to other interconnections. However, the number of sensors and switches isa vital aspect that needs to be considered when dealing with REA in PV architectures [38]. Practically, almost all of the reconfiguration techniques based on the TCT scheme require an incredible number of switches and sensors [39]. The proposed electrical array reconfiguration technique based on the TCT scheme seemsto use quite a complex control algorithm to turn switches on and off, which often requires impractical calculations [39]. Therefore, based on the author's knowledge, TCT topology cannot be reliable, effective, oreasily controlled, since it also involves complex electrical wiring. Besides this, the initial capital cost of installation, enabling practical utilizationfor commercialization, is higher.

Some researchers, such as [32,34,35,37], introduced the PV array reconfiguration method by reconfiguring the electrical wiring using two disparate parts:the fixed part and the adaptive switching control part. The yielding of optimal energy by a static electrical configuration under uncertain PS conditions is not guaranteed. Therefore, the previous researchers proposed a reconfiguration method that involved an adaptive part, for dispersing the shading throughout each shaded panel in the static part. Generally, this REA method, contrary to the electrical reconfiguration of PV arrays, is determined by the short current generated by each row of strings. This solution is controlled by the current variation index, called the CVI, to determine the best configuration, which is chosen based on the smallest CVI produced. As such, each row of the PV arrays in both the adaptive and static parts requires current sensors. However, this technique lacks criteria that might contribute to maximum power extraction due to the limitated possibility, caused by the fixed and adaptive parts, of reconfiguration achieving the highest possible maximum output power under numerous shading patterns. Thus, this technique is not applicable for maximizing the energy yield in REA implementation. Figure 7 is an example of a possiblearchitecture for the reconfiguration technique that involvesthe adaptive and static parts proposed by the previous researcher.

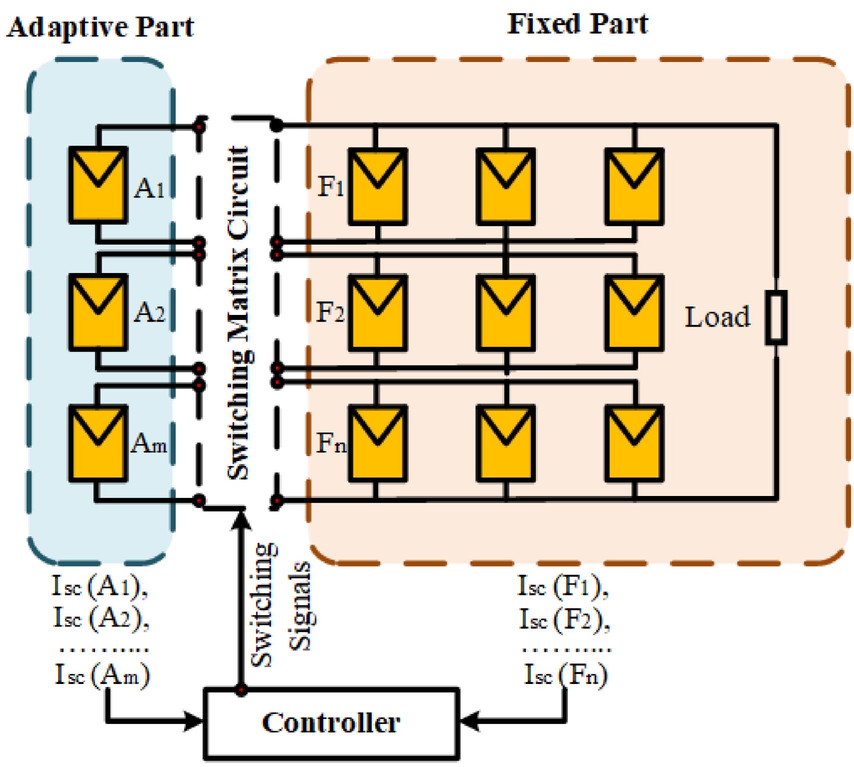

Figure 7. The block diagram of the REA method, based on an adaptive part and a static part, proposed by previous researchers.

Moreover, previous researchers have proposed alternate solutions, such as [7,33], by changingthe PV arrays' physical locationwithincertain shading patterns, based on the Sudoku dispersion rule, as shown in Figure 8.

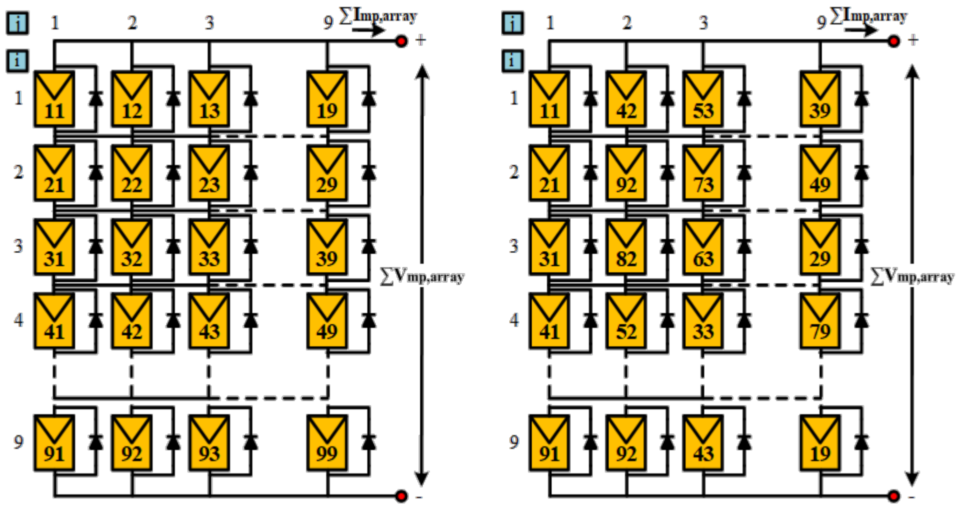

Figure 8. (**a**) TCT topology and (**b**) physical relocation of TCT scheme based on Sudoku puzzle pattern.

Undeniably, the Sudoku arrangement technique significantly increased the PV characteristic and produces higher output power under shading conditions [40]. Still, this method has a few drawbacks, such as the imprudent length of the wires for the reconfiguration process and the demandingly physical laboriousness of the relocation of the PV panels. Thirdly, this technique has some limitations, as it can only be applied for a 9 × 9 array size of PV arrays. The alteration process also does not occur in the first column of the PV arrays. As such, this shortcoming causes a reduction in the PV arrays' output power, and multiple peaks might arise due to the shaded panel on the first column remaining undispersed [17]. As discussed, this technique has some technical downsides that contribute to unfavorable system reliability.

This paper will focus on the REA method of PV arrays based on a metaheuristic evolutionary algorithm, in which FA is utilized as an optimization tool. The PV array reconfiguration will be fully utilized based on SP interconnection. The SP interconnection is widely and more practically implemented in the industry surrounding PV systems due to the smaller amountelectrical wiring and the lower complexity. As such, its initial capital installation cost is significantly lower compared to the TCT scheme. In this work, the SP topology concerning 3 × 3 arrays will be tested using MATLAB Simulink software under numerous uncertainty shading patterns and partial shading scenarios, in order to minimize the shading effects and increase the PV array's power production. The REA method implemented in this paper involvesusing a switching matrix controller as the reconfiguration circuit to equally disperse the shading pattern throughout each solar module by reconfiguring the electrical wiring of the solar modules without changing the physical location. This method is undertaken to ensure that the nearest optimal configuration is achieved for each shading profile. Also, a significant improvement in the PV system's efficiency and energy yield is expected using the proposed method.

2. System Description

2.1. Mathematical Modeling of Solar Module

Mathematical modeling is a vital aspectofthe optimal simulation design of the PV array under PS profiles. Thus, in this paper, a process of PV module modeling in MATLAB

Simulink® (Santa Clara, CA, USA) is developed based on the mathematical model of a single diode circuit diagram, which will be explained in this section. A solar panel mathematical model is built, starting from a solar cell based on a single-diode circuit diagram's simple architecture, as shown in Figure 9 to illustrate the solar panel's basic characteristics.

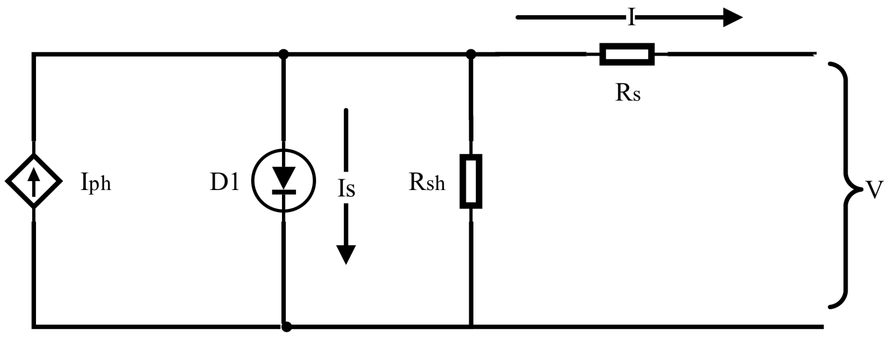

Figure 9. Single-diode equivalent circuit diagram of a solar panel.

The computational and implementational complexity increase depending on the number of parameters used for the solar cell model to improve solar panel accuracy [41]. A five-parameter model, as shown in Figure 9, is made compatible with microcontroller elaboration by considering the accuracy and calculation time, as mentioned by [39]. Based on [39], the total module current, I, composed of numerous solar cells connected in series, is expressed as

$$I = I_{ph} - I_s\left[e^{\left(\frac{V_{oc}+IR_s}{N_s m V_t}\right)} - 1\right] - \frac{V_{oc} + IR_s}{R_{sh}} \tag{1}$$

$$V_t = \frac{kT_c}{q} \tag{2}$$

where I_{ph}—photo-generated current; I_s—saturation current; Q—electron charge (1.602×10^{-19} C); V_{oc}—open circuit voltage; R_s—series resistor; R_{sh}—shunt resistor; N_s—number of series-connected cells; M—diode ideal factor; K—Boltzman's constant (1.38×10^{-23}); V_t—thermal voltage; T_c—cell temperature.

The parameters in Equations (1) and (2) need to be quantified, as they depend on the temperature and solar radiation. At the same time, the ideal factor, A, is a constant value that is independent of the surrounding temperature. The recombination type in a solar cell and the junction qualityare measured by the parameter value [42]. Furthermore, I_s and I_{ph} are the temperature-dependent parameters, and can be calculated by using the equation below.

$$I_s = I_{ds}\left(\frac{T_c}{T_{c,stc}}\right)^3 \exp\left[\left[\frac{qE_g}{Ak}\left(\frac{1}{T_{c,sts}} - \frac{1}{T_c}\right)\right]\right] \tag{3}$$

where I_{ds} is the reverse saturation current under STC, while E_g is the band-gap energy in (eV), which can be calculated as follows:

$$E_g = 1.16 - 7.02 \times 10^{-4} \frac{T_c^2}{T_c + 1108} \tag{4}$$

The photo-generated current, I_{ph}, is expressed by using Equation (5).

$$I_{ph} = \left(\frac{G}{G_{stc}}\right)\left[I_{ph,stc} + \mu I_{sc}(T_c - T_{c,sts})\right] \tag{5}$$

where in G—solar radiation (W/m^2); G_{stc}—solar radiation under STC (1000 W/m^2); $I_{ph,stc}$—photo-generated current under STC; $T_{c,stc}$—cell temperature at STC (25 °C or 298.15 K); μ_{Isc}—short current temperature coefficient; T_c—cell temperature.

Two methods can be used for the model parameters' calculation: the analytical parameters extraction and the iterative numerical calculation [43,44]. Meanwhile, substitutingEquation (5) into (1), the expression following can be obtained:

$$G = \frac{G_{sts}}{I_{ph,sts} + \mu I_{sc}(T_c - T_{c,sts})}\left[I + I_s\left[e^{\left(\frac{V_{oc}+IR_s}{N_s m V_t}\right)} - 1\right] - \frac{V_{oc} + IR_s}{R_{sh}}\right] \tag{6}$$

Equation (5) establishes an accurate method for the estimation of solar irradiation received by the solar module based on the temperature, voltage, and current measurement; besides this, the other terms are fixed, and these can be obtained from the datasheet. Also, two parameters can be used for the solar irradiation estimation. Firstly, temperature can be used in the following two cases:

(a) The PV module can be situated in an open circuit, where the V_{oc} is attained, as presented by [35];
(b) The PV module can be set in a shortcircuit, and the I_{sc} is obtained, as presented by [45].

For the two cases, the solar irradiation can be respectively calculated, as below:

$$G = G_{stc} e^{\frac{V_{oc} - V_{oc,stc} - \mu V_{oc}(T_c - T_{c,stc})}{N_s A k \frac{T_c}{q}}} \tag{7}$$

$$G = \frac{G_{stc}}{I_{sc,stc}}(I_{sc} - \mu_{Isc}(T_c - T_{c,stc})) \tag{8}$$

where $I_{sc,stc}$ is the short current under STC, while μ_{Voc} is the temperature coefficient of the opencircuit voltage. Equations (6)–(8) represent three techniques to estimate the solar irradiation, which is the vital input for the REA system's controlling algorithm. The PV module model used in this paper is JINKO JKM 280M-96. The PV module's characteristics mentioned above are presented in Table 2, based on the solar panel's datasheet.

Table 2. JINKO JKM 280M-96 module's characteristics.

Parameters	Value
Maximum power (P_{max})	280 W
Open circuit voltage (V_{oc})	63.4 V
Short circuit current (I_{sc})	5.89 A
Voltage at maximum power point (V_{mp})	52.4 V
Current at maximum power point (I_{mp})	5.34 A
Cells per module	96
Photo generated current (I_{ph})	5.9184 A
Diode saturation current (I_s)	4.7452×10^{-10} A
Temperature coefficient of I_{sc} (μ_{Isc})	0.05%/°C
Temperature coefficient of V_{oc} (μ_{Voc})	−0.29%/°C

2.2. Firefly Algorithm (FA) Application in the Proposed REA Mechanism

Based on [46,47], the FA is a metaheuristic evolutionary algorithm employed in the optimization of PV system applications, and was inspired by firefies' behavior. The model seems to be better in terms of efficiency and performance for achievingmaximum power extraction from the PV arrays under any shading circumstances, compared to the traditional PSO technique.

Basically, in nature, fireflies will mostly generate a unique short and rhythmic flashing lightvia a process called bioluminescence. Common firefly behaviorsinclude hunting, warning their enemies, mating, and communicating, and these are undertaken using a light attractiveness chemical process. This flashing light may attractother fireflies toward the brightest flashing light over various distances.

In the FA application, as an optimization metaheuristic algorithm, three idealized rules were utilized. Firstly, since all fireflies are unisex, they are attracted based on the other fireflies' brightness intensity. In a real-life circumstance, light is absorbed with a constant light coefficient $(\gamma) \in (0, \infty)$ As such, the equation can be written in the Gaussian form, as Equation (9), to calculate the fireflies' attractiveness.

$$\beta(r) = \beta_0 e^{-\gamma r^2} \tag{9}$$

The second idea is that the fireflies' brightness is different at certain distances. Assuming j and i are two different fireflies inrespectively different locations, X_i (x_i, y_i) and X_j (x_j, y_j) are their current positions. Therefore, by applying an equation based on Euclidean geometry, the distance (r_{ij}) between the two fireflies can be calculated using Equation (10).

$$r_{ij} = \|X_i - X_j\| = \sqrt{(x_i - x_j)^2 - (y_i - y_j)^2} \tag{10}$$

The less bright fireflies will be encouraged to move toward the brighter ones. Thus, the movement of firefly i attractedto firefly j can be calculated as follows:

$$X_i' = X_i + \beta_0 e^{-\gamma r^2}(X_j - X_i) + \alpha\left(rand - \frac{1}{2}\right) = X_i + \beta_0 e^{-\gamma r^2}(X_j - X_i) + \alpha \in_i \tag{11}$$

where β is the attractiveness or intensity of the firefly's flashing light, β_0 is the attractiveness at zero distance, r_{ij} is the distance between two fireflies i and j, i and j are the locations of the fireflies, X is the location of the firefly, X' is the new location of the firefly, γ is the light absorption coefficient of a given medium, α is the randomization parameter, $\alpha \in [0.1]$, and $\in_i$ is a uniformly distributed random number in [0, 1].

Thirdly, this FA can be defined similarly to theGA in terms of fitness function, since the objective function affects the brightness. The algorithm developed in this paper is based on FA, as follows. Firstly, the developed algorithm is based on either the solar panels' quantity or thearray size of the PV arrays to determine the firefly population's size. The algorithm developed will go through several iteration processes to track the highest possible G_{MPP} generated by the different switching patterns under each partial shading condition (PSC). Each completed iteration process represents the firefly population, and the highest G_{MPP} found in each population indicates the best value of the population.

Equation (10) is used to calculate the differences in the highest power co-efficients between the populations, that is, X_i, which is the previous best result of the G_{MPP} tracked for the previous population. Meanwhile, X_j is the current best result of the G_{MPP} based on the current population. Then, suppose the previous value of G_{MPP} is lower than the current best value of G_{MPP}. In that case, Equation (11) is deployed to attract the previous lower value of G_{MPP} towards the current best value of G_{MPP} based in the current iteration process. Suppose the attracted G_{MPP} of the previous population is higher compared to the current best value of G_{MPP}. Then, the algorithm will update the highest G_{MPP} with the switching patterns that generated the highest G_{MPP} value. Figure 10 clearly indicates the flowchart of the FA.

2.3. Proposed REA Mechanism Application-Based SP Interconnection

The REA-based SP scheme aims to ensure similar irradiance dispersion levels throughout all of the strings connected in series, and then to connect all of the series-connected PV arrays in aparallel configuration. By employing this technique, equivalent shade dispersion may be achieved, and the shaded PV modules will not become a limitation of the current generated for the PV module with higher irradiance exposure in the same series string, as presented by [37]. Figure 11 shows the proposed switching matrix architecture that has been connected with solar panels. As an alternative for the REA technique applied, this paper will focus on experimental analysis and evaluation to improve the PV arrays' efficiency and performance under mismatch circumstances by utilizing the SP interconnection with an array size of 3 × 3 (Figure 12).

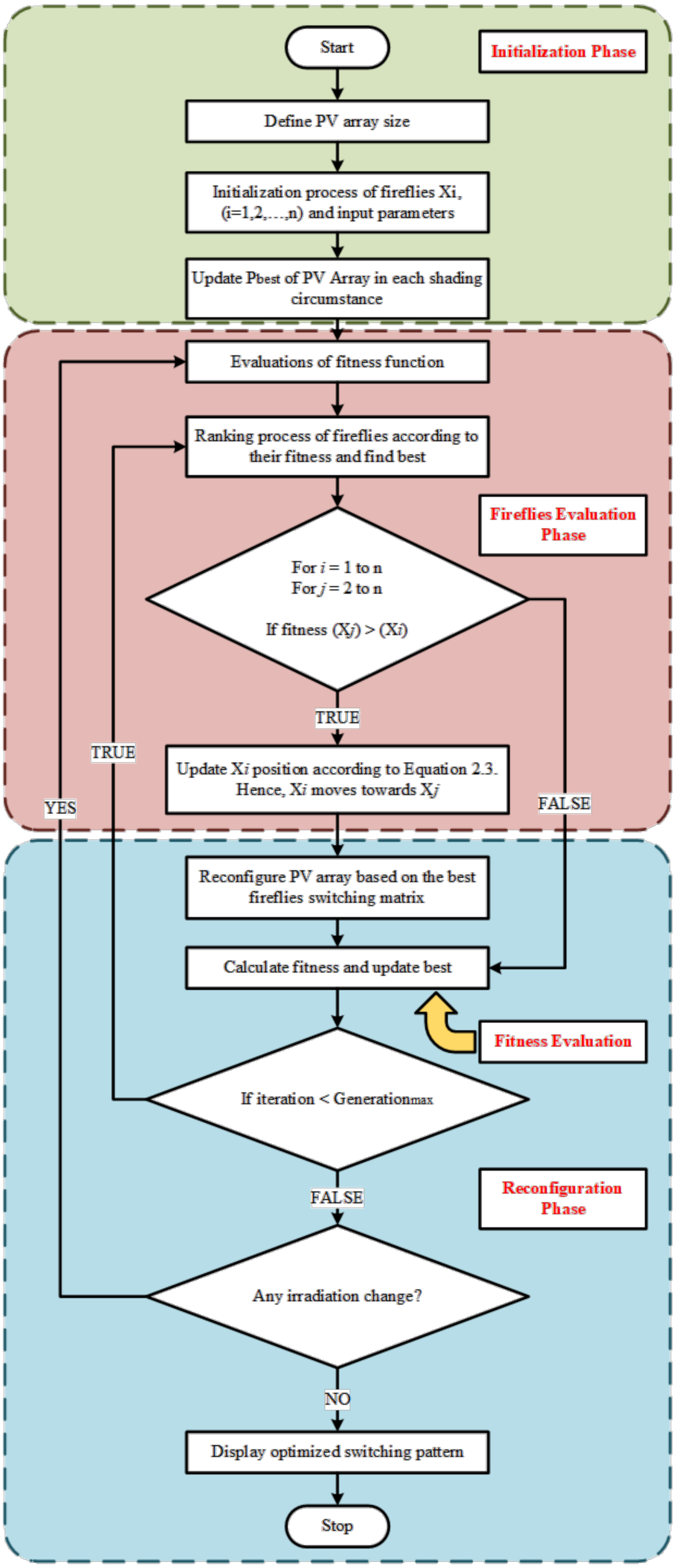

Figure 10. Flowchart of the proposed firefly algorithm (FA).

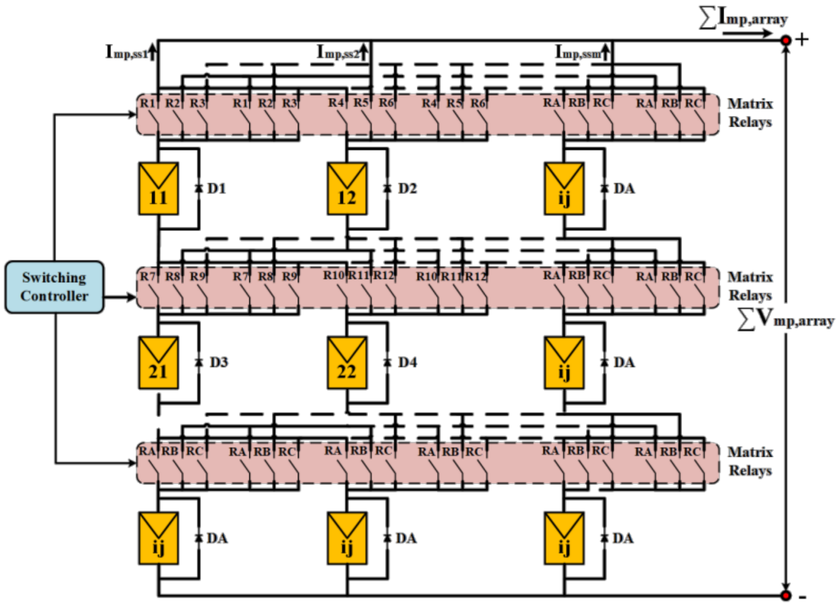

Figure 11. The proposed REA technique for SP topology with a $i \times j$ array size.

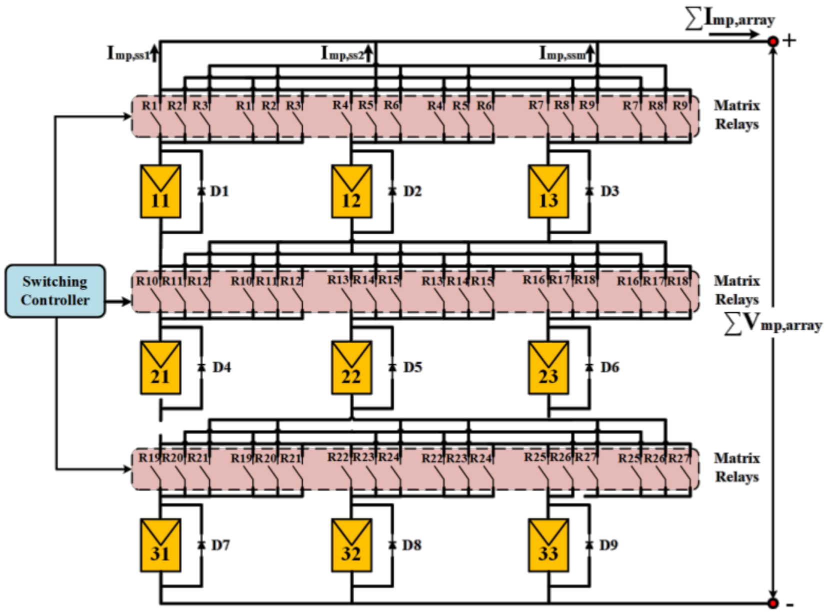

Figure 12. Proposed REA technique for the applied 3 × 3 array size.

For the REA method proposed in the SP application, a double pole double through (DPDT) relay was used for the switching matrix configuration, instead of other semiconductor switches, such as MOSFET transistors. However, the semiconductor switches that are incontestable can operate at a very fast switching frequency for a faster convergencespeed, thusenabling them to obtain the switching matrix that produced the highest G_{MPP} faster. Still, the contact of the relay has zero closed resistance. Meanwhile, the semiconductor switches showa reduction in forward voltage, which can lead to energy losses. The relay also can operate at an extreme temperature compared to the other semiconductor switches. It can easily troubleshoot for the hardware's implementation due to its normally closed (NC) and normally open (NO) mechanical characteristics, besides its plug and play characteristics. The total number of switches for *PV* modules, $\sum SW_{DPDT}$, utilized in the proposed REA is based on the array size, $i \times j$, or the total number of series strings, $\sum N_{ss}$, and the total number of PV modules, $\sum N_{PV}$, connected in the SP interconnection. The expression for $\sum SW_{DPDT}$ is as follows:

$$\sum SW_{DPDT} = \sum N_{ss} \times \sum N_{PV} \tag{12}$$

Moreover, the total connected number of switches for each PV module, $\sum SW_{PV,\,DPDT}$, is dependent on the $\sum N_{ss}$ only, and can be expressed as in Equation (13).

$$\sum SW_{PV,DPDT} = \sum N_{ss} \tag{13}$$

Since the 3 × 3 array size is implemented in this paper, and the $\sum N_{PV}$ connected is 9PV modules, the $\sum SW_{DPDT}$ for the presented PV array size is 27, the $\sum SW_{PV,\,DPDT}$ is 3, and the switching matrix architecture for the applied array size is demonstrated in Figure 12.

Based on [48,49], the V_{mp} and Imp of a single PV module can be calculated using Equations(14) and (15).

$$V_{mp} = V_{mp,stc} + [\mu_{Voc}\,(T - T_{stc})] \tag{14}$$

$$I_{mp} = I_{mp,stc} \times \frac{G}{G_{stc}} \tag{15}$$

where V_{mp}—voltage at the maximum power point; $V_{mp,stc}$—voltage at the maximum power point under STC; μV_{oc}—temperature coefficient of Voc; Tc,stc—cell temperature at STC (25 °C or 298.15 K); Tc—cell temperature; I_{mp}—current at the maximum power point; $I_{mp,stc}$—current at the maximum power point under STC.

Then, after the V_{mp} and I_{mp} of a single PV module are obtained for each shading circumstance, Kirchhoff's law is applied for the voltage summation in the series string and the current summation of the parallel connection to calculate the PV arrays' P_{mp} for each shading profile. The total array voltage at the maximum point, $\sum V_{mp,array}$, for the PV array size applied in this paper is calculated using Kirchhoff's voltage law (KVL), as in Equation (16). Meanwhile, the total array current for the parallel connection, $\sum I_{mp,array}$, is calculated using Kirchhoff's current law (KCL), as in Equation (19).

$$\sum V_{mp,array} = \sum_{n=ij}^{ij} V_{mp,ij} \tag{16}$$

In Equation (16), $V_{mp,ij}$ indicates the V_{mp} of the specific PV module in the arrays, whereas "n" is the number of PV modules, "i" indicates the number of rows, and "j" indicates the number of columns for the PV module's location in the series string. The total number of columns and rows in the specific PV array depends on the array size matrix. For example, in this case, the KVL expression will be as follows:

$$\sum V_{mp.array} = V_{mp,11} + V_{mp,21} + V_{mp,31} \tag{17}$$

In the KVL theory, the total voltage for every series string at the maximum power point, $\sum V_{mp,ss}$, in the parallel connection is equivalent. Consequently:

$$\sum V_{mp.array} = V_{mp,SS1} + V_{mp,SS2} + V_{mp,SS3} \tag{18}$$

Meanwhile, KCL is applied to calculate $\sum I_{mp,array}$. It is based on the total current produced by each series string, $I_{mp,ss}$, at the maximum point, as shown in the calculation, whereas "m" in the equation indicates the number of series strings.

$$\sum I_{mp,array} = \sum_{m=1}^{m} I_{mp,m} \tag{19}$$

According to the applied array size, the expression is as displayed in Equation (20). Lastly, the overall maximum power of the PV array produced for certain PS profiles, $\sum P_{mp,array}$, is calculated by using Equation (21).

$$\sum I_{mp.array} = I_{mp,SS1} + I_{mp,SS2} + I_{mp,SS3} \quad (20)$$

$$\sum P_{mp,array} = \sum V_{mp,array} \times \sum I_{mp,array} \quad (21)$$

In terms of the real hardware prototype development cost, the proposed REA for a 3 × 3 array with 4 kW capacity is estimated to be around USD 1850. The three main components ofthe hardware prototype are (1) a solid-state relay, (2) a controller, and (3) a capacitor-based I–V curve tracer. Since a high-power solid-state relay is expensive, the proposed technique's total cost closelydepends on the size and capacity of the developed system. As discussed earlier, for 3 × 3 arrays, 27 relays are required. The number of relays will increase with the size of the array. For a controller, the Texas Instruments TMS320F28335 DSP controller, or any suitable controller, can be employed. This controller is used to control the switching of the relay and the I–V curve tracer. During each combination of relay switches, the maximum output power will be determined through the I–V curve tracer, and the algorithm employs this information to guide the FA particle towards the best switching combination.

The proposed method is suitable for small- to medium-scaled PV systems. The reconfiguration solution is certainly more suitable for PV systems installed in the area, where frequent cases of partial shading occur during only some parts of the day. For example, in the case of shadows (caused by poles, small walls or buildings), which occur only at sunrise and/or sunset, during the central part of the day, the PV field works without mismatching.

2.4. Analysis of Partial Shading (PS) Profiles

As explained in the introduction, the solar module absorbs the photon energy received by the sunlight and converts it into direct current by creating the potential difference and allowing the movement of electrons in the p–n junction of the solar module. This process is called thephotovoltaic effect, which refers to the production of power in the material due to exposure to sunlight. The dispersion of the assorted irradiance values and shading patternsreceived by the PV arrays from sunlight will contribute to the performance and efficiency of the power coefficient produced by PV arrays. The irradiance value exposed to each solar module will affect the current produced. Thus, the solar module's current will significantly increase if the shading is exposed to a higher irradiance value, emitted by sunlight towards the solar module.

Consequently, the PV array's behavior under miscellaneous PS profiles has been tested in MATLAB Simulink® software to fully employ the proposed REA technique. The experimental analysis and evaluation are intended toenhance thePV arrays' performances by applying the REA technique during mismatch conditions. For the implementation of the proposed REA technique, the value of the irradiance or shading patterns directedtoward each PV module has been varied for each scenario, as displayed in Figure 13. The variation in irradiance values isbetween 1000 W/m^2, 700 W/m^2, 500 W/m^2, and 300 W/m^2. Meanwhile, the surrounding environmental temperature is constant at 25 °C, since the temperature only has a minor effect on the PV array's behavior during mismatch conditions.

2.5. Analysis of PV Arrays and the Proposed REA Technique under Mismatch Profiles

To evaluate and analyze the suitability of the developed FA implemented with the proposed REA method, a comprehensive test had been performed under heterogeneous PSC, as shown in the previous chapter. The same test conditions were maintained forthe SP interconnection and the TCT, with the same array size, in order to evaluate, analyze, and quantitatively compare the proposed technique's overall performance and efficiency in improving the PV array system's efficiency, with different shading strength (SS) values.

Based on the experimental analysis performed, the FA algorithm applied with the REA technique showed positive results, since the technique completely overpassed the overall performance of the standard SP configuration applied in real-life industry. Meanwhile, the proposed method's power coefficient also exceeds the conventional TCT scheme's powerunder all conditions. Table 3 shows the SP scheme's overall performance comparison, the TCT scheme, and the FA applied with the REA technique under all of the PSC.

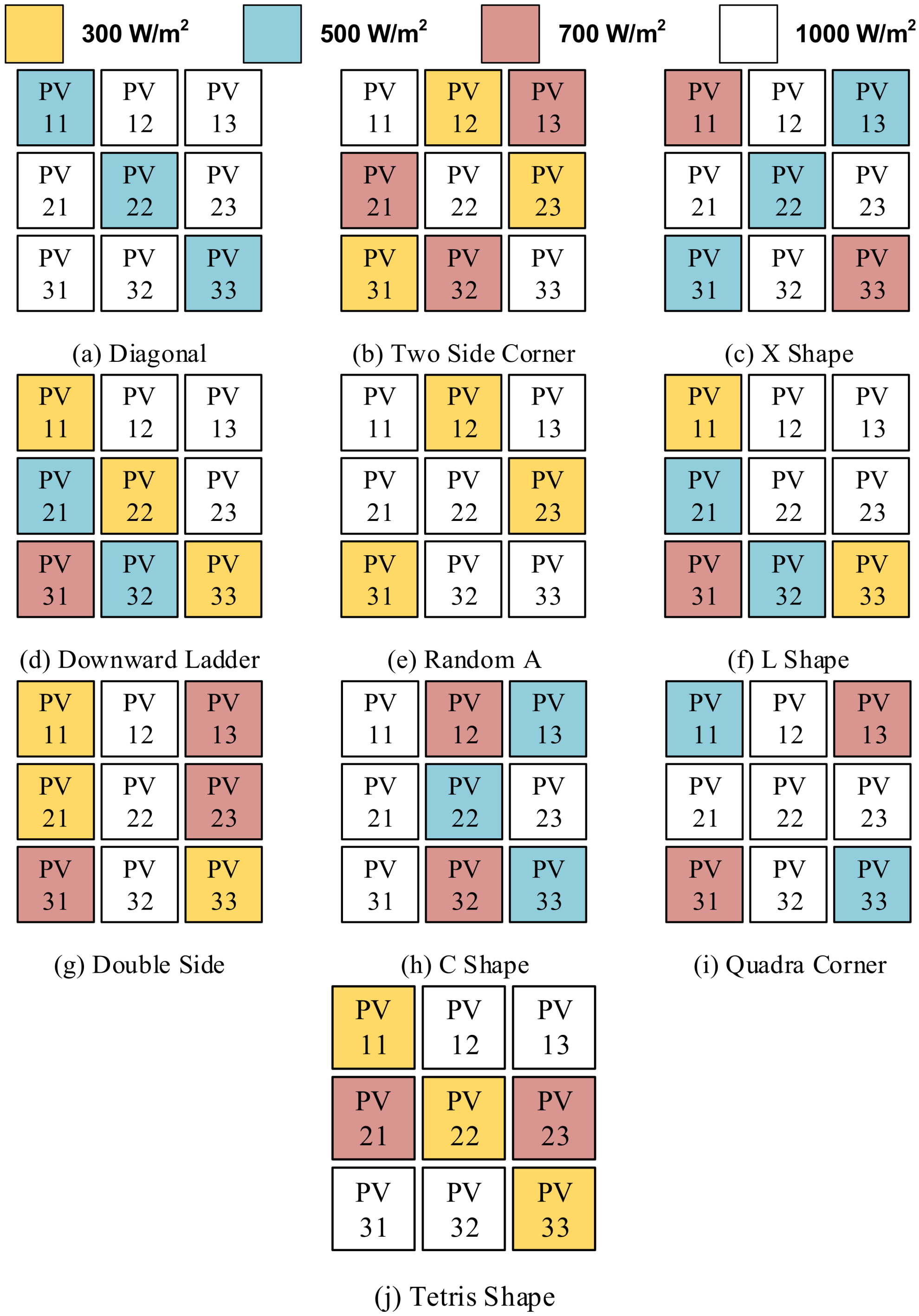

Figure 13. Partial shading (PS) patterns for the simulation of the experimental analysis and evaluation of the proposed REA method in the MATLAB Simulink® software.

Table 3. A comprehensive comparison of the overall performance under various PSC.

Conditions	MPP, W			Shading Strength (SS), %	Improvement Efficiency with SP Scheme, %
	Series–Parallel (SP)	TCT	FA		
Downward Ladder	938.2692	1123.0762	1155.1823	37.78	23.12
L Shape	1147.9575	1145.1144	1175.9137	22.22	2.43
Quadra Corner	1433.161	1582.0201	1654.1853	17.78	15.42
Random A	1362.56	1585.0017	1670.6502	23.33	22.61
Tetris Shape	1130.3715	1276.0748	1314.6883	30.00	16.31
Triangle Shape	1151.6012	1191.6321	1552.9542	22.22	34.85
Two Side Corner	1022.8226	1381.4238	1449.9129	33.33	41.76
U Shape	1113.2946	1429.1947	1491.8086	27.78	34
X Shape	1154.2603	1558.6239	1633.0891	23.33	41.48
X (500) Shape	1113.2959	1429.1945	1491.8317	27.78	34

The shading strength (SS) of each PSC for experimental analysis purposes, depended on each PV panel's shading pattern and calculated using Equation (22). The SS of the experimental analysis performedis about 15 to 40%, as isstated in Table 3 for all PSC.

$$SS(\%) = \frac{\sum irradiance_{STC} - \sum Irradiance_{PSC}}{\sum irradiance_{STC}} \times 100\% \quad (22)$$

where $\sum Irradiance_{STC}$ is the summation of the irradiance's value under standard test conditions, and STC is 1000 W/m^2 for all of the PV panels. Since, for this case, the applied array size is 3×3, the total number of PV panels is nine, and the $\sum Irradiance_{STC}$ is equal to 9000 W/m^2. Meanwhile, $\sum \mathrm{Irradiance}_{\mathrm{PSC}}$ is a summation of the irradiance directedtoward each PV panel under PSC. Below is an example of the SS calculation for the Downward Ladder scenario.

$$\sum Irradiance_{PSC} = 3(1000) + 3(300) + 2(500) + 700 = 5600\, W/m^2 \quad (23)$$

Therefore, the SS (%) for the Downward Ladder scenario is as follows.

$$SS(\%) = \frac{9000\, W/m^2 - 5600\, W/m^2}{9000\, W/m^2} \times 100\% = 37.78\% \quad (24)$$

Based on the experimental analysis performed, it can be seen that the SS value of the PSC is one of the factors that will affect the energy efficiency improvement of the PV arrays achievedusing the REA method equipped with FA, as compared to the conventional SP configuration. In contrast, the REA method is hypothesized to become more effective when the SS is higher. For example, during the Two Side Corner scenario, the SS value is the second highest, at 33.33%, resulting in the highest energy improvement efficiency, which is 41.76%. However, some cases depend on the shading pattern itself, and the domain factor of the limitation of the current produced, caused by the shaded PV panels in the series strings under each PSC, which can contribute to a more efficient power coefficient improvement; for example, the X Shape and Random A patterns. Even though the X Shape and Random A conditions possess the same SS value, which is 23.33%, the X Shape's power coefficient improvement is greater than the Random A's; 41.48% for the former and 22.61% for the latter. This happens due to the limitation of the current produced by the shaded PV panels' domain factor in each series string under the SP scheme, and the shading pattern itself during the X Shape scenario. The REA technique equally dispersed the X Shape scenario's shading pattern by reconfiguring the PV arrays' topology. As such, the proposed method's energy efficiency improvement for the X Shape condition is comparable to that of the standard SP topology and the Random A scenario, which both possessed a less complex shading pattern.

The power improvement yield also depends on the PSC patterns' complexity in reconfiguring the PV arrays. Suppose the complexity of the PSC is more complex. The possibility of energy coefficient improvement is higher than with the less complex PSC pattern, such as in the X Shape scenario, the Triangle Shape scenario, and the Two Side Corner scenario, which all result in a higher G_{MPP} being produced. As such, as a result, when the complexity of the PSC is increased, the possibility of the proposed FA and REA technique being more effective in power coefficient improvement is also increased. Figure 14 shows acomparis on of the P–V curves for each PSC scenario for the SP topology, the TCT topology, and the proposed REA technique.

From the P–V curves, we can see that the proposed REA solution successfully solved about 70% of the multiple peaks problems due to the limitation currently imposed by the shaded solar panels in the series string of the SP topology under PSC, which can cause areduction in power yield production. Furthermore, the REA method also successfully increased the PV arrays' power output compared to the TCT interconnection. The proposed REA technique reconfigured the electrical wiring scheme of the PV array under each PSC by controlling the switching pattern of relays. The relays for the proposed REA technique are turned on and off by a digital number, i.e.,"0" and "1". The developed FA will create various numbers for switching the matrix variables (VARs) patterns for every PSC based on the population's size, as determined by the FA. To control the relays within an array of 3×3 size, as applied in this research, a set of the following coding is essential to determine which relays turn on under certain conditions.

The set number of VARs for the proposed FA is based on the columns or series strings of PV arrays. Since the applied array size of the PV arrays for this research is 3×3, then the set numbers of VARs are 1, 2, and 3 for each solar panel. If the applied array size is 5×5, then the set number of VARs is 1, 2, 3, 4, and 5, to determine which relay is activated for each PV panel in the PV system. Thus, the best VAR, VAR_{Best}, found under each PSC tested for this project is presented in Table S1. Based on Table S1, if the number of VAR_{Best} is 1, case 1 in the following coding will be utilized to turn on relay 1; if the number of VAR_{Best} is 2, case 2 will be used to switch on relay 2, and if the number of VAR_{Best} is 3, relay 3 will be activated by case number 3. Each solar panel's switching pattern in the PV arrays under the proposed REA method is controlled by each number in the set of VAR arrays. For example, the set number of VAR_{Best} for the Downward Ladder scenario is "1 2 3 1 1 3 2 3 2". The first number of VAR1 is 1, which is used to determine which relay is turned on for PV11 solar panels.

Meanwhile, VAR2 is used to determine which relay is switched on for the PV21 solar panel, and VAR3 is applied to determine which relay is activated for the PV31 solar panel. The same condition is also applied to other VARs. Figure 15 is the arrangement of the VAR in the proposed REA technique.

Table S2 shows the state of relays for each PSC, which are normally closed (NC), representing that the relay is activated, andnormally opened (NO), representing that the relay is deactivated, based on the set number of VAR_{Best} generated for each PSC. Based on Table S2, it can be seen that each PSC has a different set of switching patterns, depending on the PSC, directed towards the PV arrays in order to track the highest possible G_{MPP}.

As for the Downward Ladder scenario, the set of VAR_{Best} is "1 2 3 1 1 3 2 3 2". Since VAR1 is 1, relay 1 is activated and reconnected via the electrical wiring of PV11 with the first column and second column of the series string. Meanwhile, VAR2 is 2. Thus, relay 11 is switched on, and reconnects PV21 with PV12 and PV13. Furthermore, PV31is reconnected with PV21 and PV23, since VAR3 is 3. The same condition was also applied for VAR4 up to VAR9, and other shading scenarios, so as to reconfigure the PV array's electrical wiring for the proposed REA under different PSC. Figure 16 presents a clear figure of the PV array's electrical wiring after the reconfiguration process, which accomplishestracked and triggered switching patterns that produce the highest possible G_{MPP} under each scenario.

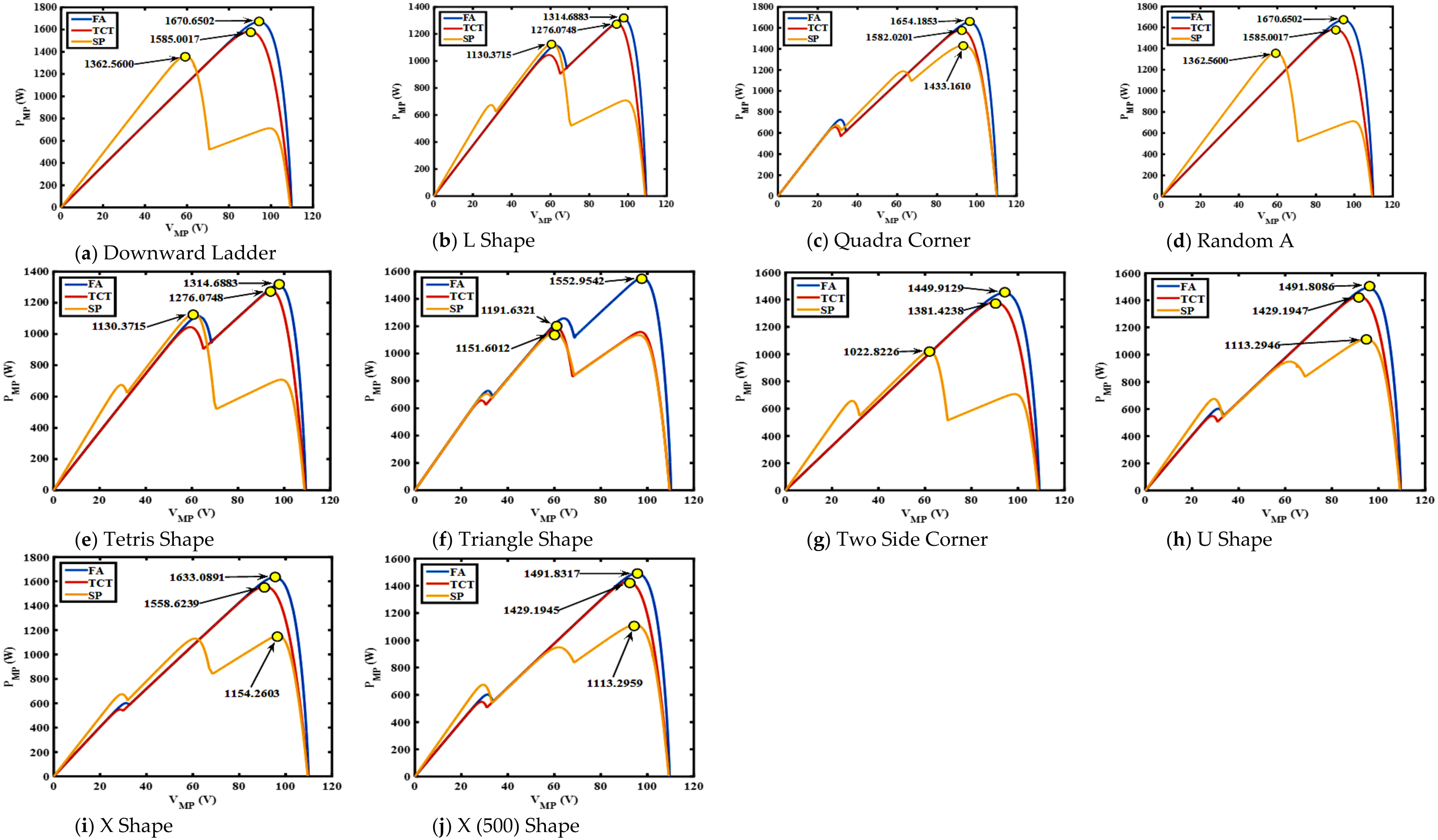

Figure 14. P–V curves of SP scheme, TCT scheme and the proposed REA method under each PSC.

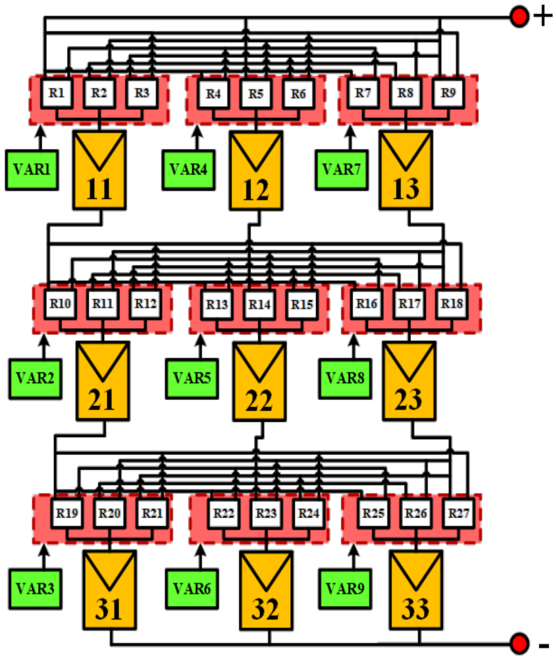

Figure 15. Variables (VAR) mapping for the proposed REA technique.

Based on Kirchhoff's current law (KCL), the series strings'produced current is limited to the lowest produced current. As a result, the activation of the P–V curve's turning point occurred, and contributed to the multiple-peaks scenario, representing the power produced by each solar panel in the series strings. Since the G_{MPP} of the PV arrays is dependent on the current and voltage produced by the solar panels, the shaded PV panels that produced the lowest current will affect greater power losses for the system under PSC, and cause the power efficiency of the PV arrays to decrease. Based on the observations and the thorough experimental analyses performed, the REA method has been proposed to reconfigure the electrical wiring of the PV arrays under each PSC, based on the shading patterns, so as to achieve equal dispersion of the solar panels' irradiance values in each series string. This is performed toresolve the multiple peaks faced by conventional SP topology due to the current limitation produced by the shaded PV panels in the series string. An equal dispersion of the irradiance pattern is successfully obtained by the proposed REA method under a PSC of about 70%, as presented in Figure 14. As a result, the technique has solved the common problem of multiple peaks faced by the standard SP scheme, and increased the efficiency of the PV arrays while reducing the power losses during PSC. Even though employing the novel TCT interconnectionas the proposed REA technique has also successfully solved the multiple peaks problem, the proposed REA technique that utilized FA as a control and optimization algorithm to track the highest global peak successfully increased the power yield of the PV arrays to a greater extent than the TCT scheme.

The FA developed for the REA technique will create numerous switching pattern populations for each iteration. The proposed algorithm will undergo numerous iteration processes to track the highest possible global peak for each PSC. The number in the population, Pop_{num}, is dependent on the array sizes or the quantity of the solar panels in the system. In contrast, the maximum number of iteration process, $Iter_{max}$, is randomly determined by the author. Therefore, for the applied 3×3 array size, the Pop_{num} of each iteration is nine, and the $Iter_{max}$ is set to 25 for this experimental analysis. The proposed method will continuously carry outthe iteration process until it reaches $Iter_{max}$. Figure 17 shows the iteration process graph of G_{MPP} convergence for each iteration, and Table 4 presents the number of iterations, $Iter_{num}$, required to achieve a steadystate in the highest G_{MPP}.

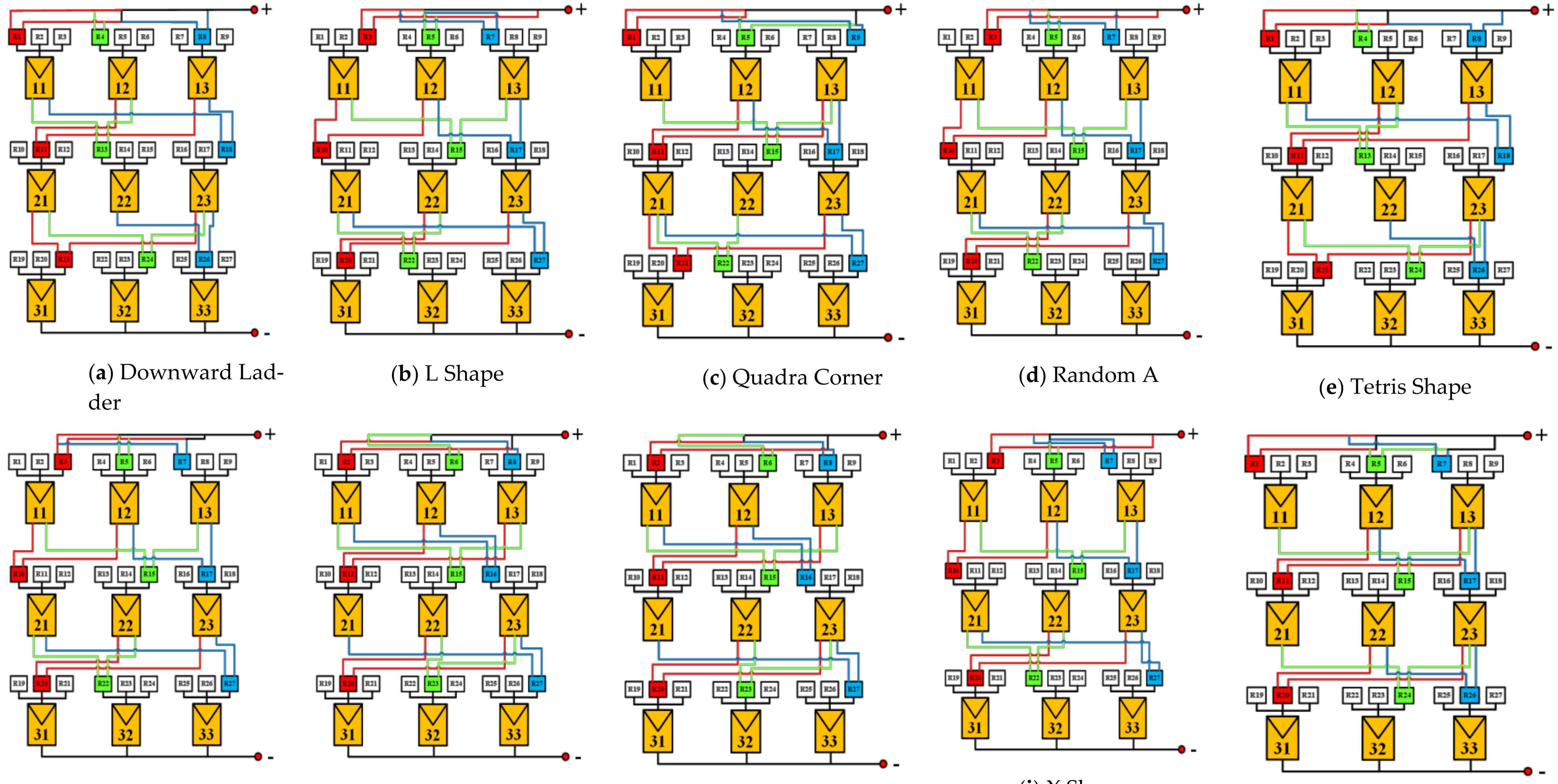

(**a**) Downward Ladder (**b**) L Shape (**c**) Quadra Corner (**d**) Random A (**e**) Tetris Shape

(**f**) Triangle Shape (**g**) Two Side Corner (**h**) U Shape (**i**) X Shape (**j**)X (500) Shape

Figure 16. Reconfiguration of electrical wiring under each PSC.

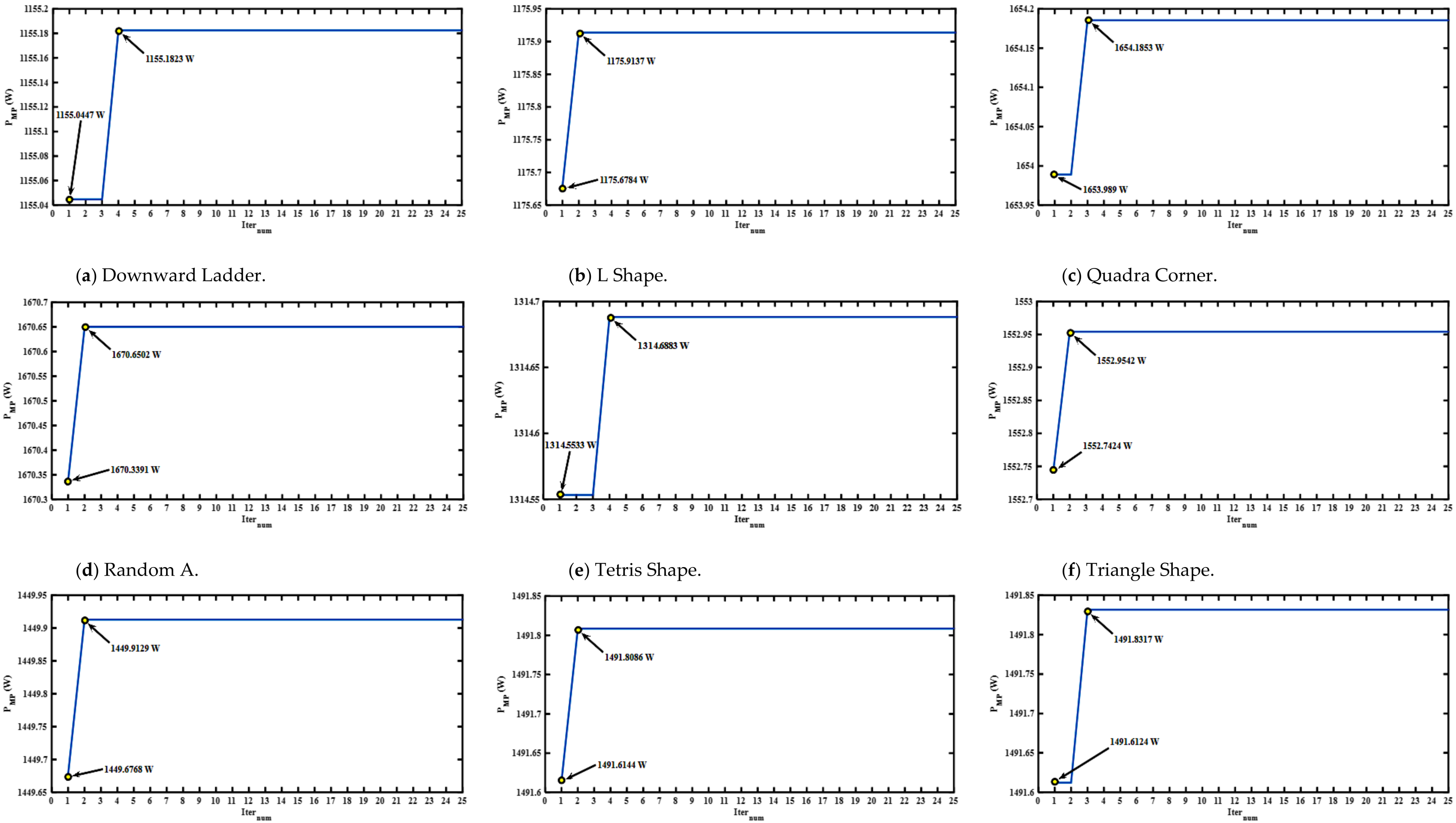

(**a**) Downward Ladder. (**b**) L Shape. (**c**) Quadra Corner.

(**d**) Random A. (**e**) Tetris Shape. (**f**) Triangle Shape.

(**g**) Two Side Corner. (**h**) U Shape. (**i**) X Shape (500).

Figure 17. G_{MPP} of proposed REA technique for each number of iterations ($Iter_{num}$).

Table 4. $Iter_{num}$ required to achieve a steady state in the highest G_{MPP}.

Conditions	$Iter_{num}$ Required to Achieve Asteady State in the Highest G_{mpp}
Downward Ladder	4
L Shape	2
Quadra Corner	3
Random A	2
Tetris Shape	4
Triangle Shape	2
Two Side Corner	2
U Shape	2
X Shape	2
X (500) Shape	3

Based on Figure 17 and Table 4, the FA developed a fast, efficient and dynamic metaheuristic algorithm to generate the switching pattern, and to optimize and track the highest G_{MPP} under each PSC. Based on the experimental analysis done, it can be observed that the steady state in the highest G_{MPP} is consistently achieved at the early stage of the iteration process, which is between iterations two and four. In almost 6 out of 10 PSCs, the steady-state highest G_{MPP} is achieved at iteration two. However, it is undeniable that the developed FA reconfigured the electrical wiring of the PV arrays ata fast convergence speed, since, based on Figure 17, the developed FA consistently initiated a switching pattern that produced a high global peak compared to the TCT topology at iteration one under all conditions. There is only a small difference-gap in the global peak, which is no more than 1 W between the previous steady-state G_{MPP} and the current steady state of the highest global peak for each iteration under all PSC.

Moreover, to thoroughly analyze the performance of the proposed method, the author has also implemented the proposed solution for a larger array size, that is, 5 × 5. This was done to comprehensively test and analyze the proposed REA technique's capacity in handling larger PV arrays. Figure 18 presents the proposed REA method with the 5 × 5 array size. The experiment's model setup for the 5 × 5 array size in the MATLAB Simulink software is similar to that of the 3 × 3 array size. Figure 19 presents the five random PSC patterns tested for the 5 × 5 array size. The Pop_{num} and the $Iter_{max}$ for the applied 5 × 5 array size were set to 25 and 20. The best of the switching variables, VARBest, under each PSC tested for the 5 × 5 array size with the proposed REA technique are given in Table S3.

Based on the P–V curves presented in Figure 20 and the data presented in Table 5, the proposed REA technique equipped with the FA can be seen to have overwhelmed the TCT scheme's performance, and the SP topology, under all PSCs tested for the 5 × 5 array size. Based on Table 5, the REA technique's efficiency improvement with the conventional SP scheme is between 3.69 and 35.35%. The power coefficient gap with the SP interconnection is between 114.5851 W and 1215.1531 W, while it achieved a 42.7013 W to 448.5455 W power yield improvement compared to the TCT interconnection. The improvement in power output achieved by the proposed REA technique for the 5 × 5 array size has shown that the method successfully reconfigured the electrical wiring of the PV arrays, which then produced ahigher G_{MPP} than the TCT interconnection did under all PSCs tested. Thus, this shows that the proposed REA technique is flexible, and able to improve the conventional static topology's performance under different PSCs by reconfiguring the electrical wiring for divergent conditions.

Based on the experimental analysis done for the 5 × 5 array size, the major factor contributing to the geater power coefficient improvement is the shading pattern. The data presented in Table 5 clearly show that even though the X (500) Shape and Triangle Shape possessed a similar value of SS, which is 18.0%, the X (500) Shape achieveda higher performance improvement, 35.35%, compared to the Triangle Shape, the improvement of which was 16.22%. A similar case also arises in the Short and Long scenario with the highest SS, which is 38.4%. Nevertheless, the Short and Long pattern is the pattern with the highest SS percentage value, but the energy boost efficiency of the REA method is only 5.31%. This happens due to the limitation of the shading pattern to be reconfigured for higher energy yield improvement. The state of the relays in the 5 × 5 array size, using the REA method under each PSC, is presented in Table S4.

Besides this, based on the analysis done, it is proven that FA is a fast and dynamical optimization metaheuristic algorithm for tracking and generating the switching pattern that produces the highest G_{MPP} under each PSC. The G_{MPP} at each iteration under each PSC is presented in Figure 21. Based on Figure 21, the highest G_{MPP} produced by the proposed REA technique under each PSC is achieved at the early stage of the iteration process. For the Downward Ladder pattern, the highest steady-state of G_{MPP} is achieved at $Iter_{num}$ 13. However, a high power yield compared to the TCT scheme is achieved at $Iter_{num}$ 2. The proposed solution generated by the switching pattern that produced a higher G_{MPP} value compared to the TCT interconnection is attained at $Iter_{num}$ 1 for the Short and Long, Triangle Shape, and L Shape patterns. In spite of this, for the X (500) Shape, the TCT scheme equally dispersed the current produced in each string. As such, the high G_{MPP} produced by the REA technique compared to the TCT scheme is procured at $Iter_{num}$ 5. Nonetheless, it is undeniable that the proposed REA method executed the switching patterns and reconfigured the PV array's electrical wiring at a fast convergence speed, thus achieving a higher G_{MPP} than a novel and widely used SP interconnection, which was obtained at $Iter_{num}$ 1 for all conditions tested. Tables S3 and S4 present the arrays of VAR_{Best} and the state of the relays that produced the highest G_{MPP} under each PSC trial.

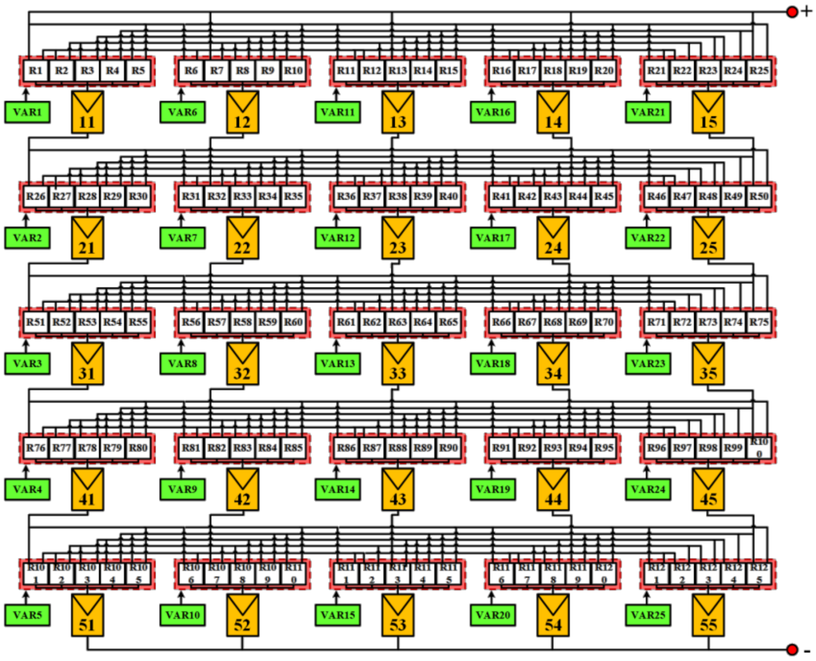

Figure 18. The REA proposed method applied the 5 × 5 array size.

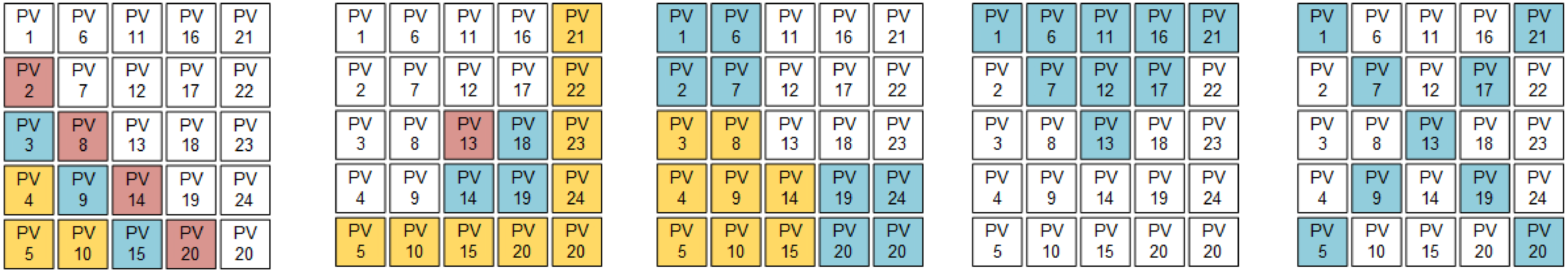

(**a**) Downward Ladder (**b**) L Shape (**c**) Short and Long (**d**) Triangle Shape (**e**) X (500) Shape

Figure 19. PSC patterns tested on 5 × 5 array size.

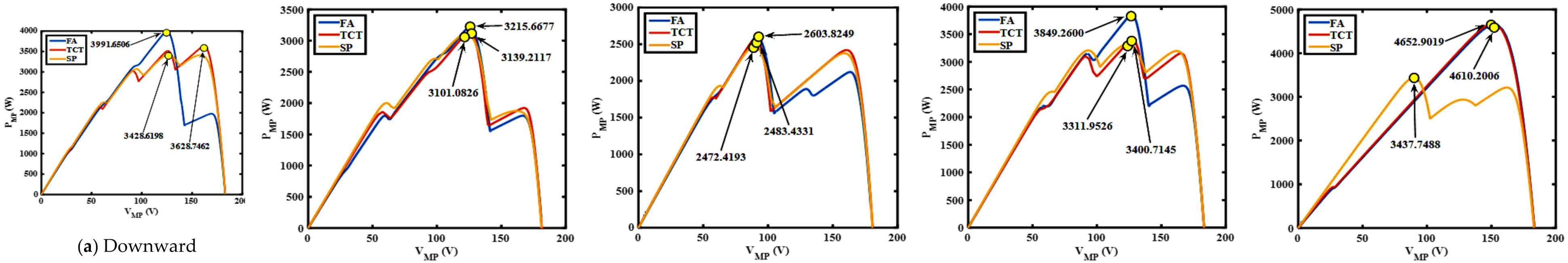

(**a**) Downward Ladder (**b**) L Shape (**c**) Short and Long (**d**) Triangle Shape (**e**) X (500) Shape

Figure 20. P–V curves of 5 × 5 array size for the SP scheme, TCT scheme, and the proposed REA method under each PSC.

Table 5. Quantitative comparison of overall performance under each PSC for 5 × 5 array size.

Conditions	MPP, W			Shading Strength (SS), %	Improvement Efficiency with SP Scheme, %
	SP	TCT	FA		
Downward Ladder	3428.6198	3628.7462	3991.6506	19.2	16.42
L Shape	3101.0826	3139.2117	3215.6677	32.4	3.69
Short and Long	2472.4193	2483.4331	2603.8249	38.4	5.31
Triangle	3311.9526	3400.7145	3849.2600	18.0	16.22
X (500) Shape	3437.7488	4610.2006	4652.9019	18.0	35.35

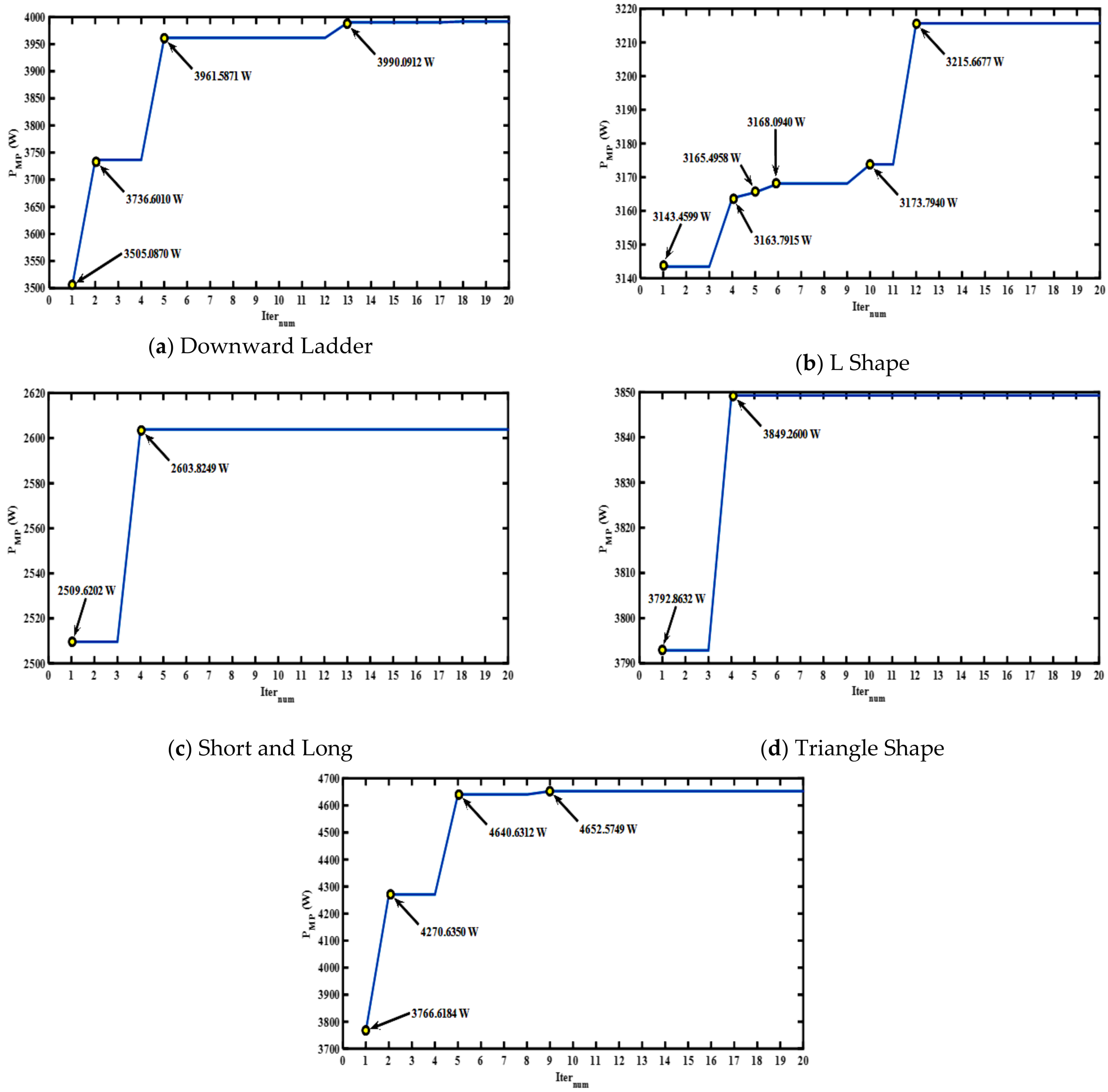

(**a**) Downward Ladder

(**b**) L Shape

(**c**) Short and Long

(**d**) Triangle Shape

(**e**) X (500) Shape

Figure 21. G_{MPP} of the proposed REA technique for the 5 × 5 array size at each $Iter_{num}$.

Finally, the proposed REA technique has wide-ranging advantages, and can also be applied in the real world for any array size. The special features of the proposed REA method are as follows:

(a) Provides an extra safety circuit autonomously, which can be controlled automatically for maintenance purposes, such as damaged PV panel replacement, if the proposed solution is further developed in the future;
(b) The proposed REA method can fully reconfigure the electrical wiring of the PV arrays' interconnection without changing the physical location of the solar panels based on the surrounding climate or partial shading conditions, in order to enhance the performance of the PV systems under uncertain environmental climate conditions and assorted shading patterns;
(c) The proposed REA approach can also reconfigure the electrical wiring by automatically disconnecting the unpredictable solar modules and reconnecting the working solar modules in the PV arrays, in order to reduce the greater energy loss caused by the non-working solar modules;
(d) The REA technique can enhance the PV system's power coefficient dynamically and ata highconvergence speed under any partial shading conditions;
(e) The proposed PVAR technique is compatible with any algorithm, such as the particle swarm optimization (PSO), genetic algorithm (GA), and differential equation (DE) algorithms, as well as any other algorithms for the further improvement and ful reconfiguration of PV systems' topology.

3. Conclusions

This paper's main objectivewas to enhance the conventional static interconnections' performance and efficiency under contrasting PS profiles. Based on the experimental analysis performed, the author can conclude that the proposed REA technique successfully improved the performance of the PV arrays under PS profiles compared to the novel SP topology and TCT scheme. The power coefficient of PV arrays wassuccessfully increased under all conditions tested. Also, the proposed REA successfully reconfigured the electrical wiring of the PV arrays under different PSCs, and tracked the highest G_{MPP} with a very fast convergence speed, since a higher steady-state in the G_{MPP} compared to the SP and TCT interconnections is achieved in the early stage of the iteration process. Furthermore, the FA utilized in this paper is efficient and easily applied or implemented in real life, since it does not involve a complex equation for the optimization process. The proposed REA solution can be applied with an algorithm for the further enhancement of PV arrays'performance. If the proposed REA technique is further developed in the future, the proposed REA technique can make the PV system a sophisticated, flexible, and efficient technology, attracting new market investors to participate, and invest more, in the PV industry. Thus, it can increase the awareness of green and clean energy in supplyingelectricity in the future.

Supplementary Materials: The following are available online at https://www.mdpi.com/2071-1050/13/6/3206/s1, Table S1: Best of Switching Variables, VARBest under each PSC tested for the proposed REA technique, Table S2: State of Relays for each PSC, Table S3: Best of Switching Variables, VARBest under each PSC tested for the 5 × 5 array size of the proposed REA technique, Table S4: State of relays for 5 × 5 array size of REA method under each PSC.

Author Contributions: Conceptualization, M.N.R.N., M.F.N.T., and T.S.B.; data curation, M.N.R.N., M.F.N.T., and N.M.K.; formal analysis, M.N.R.N., M.F.N.T., and A.A.; funding acquisition, T.S.B., M.M., N.M.K.; project administration, T.S.B., M.M., N.M.K.; investigation, M.M., N.M.K.; methodology, M.N.R.N., M.F.N.T., and A.A.; resources, T.S.B., M.M., and N.M.K.; software, M.N.R.N., M.F.N.T., A.A., and T.S.B.; visualization, N.M.K., T.S.B.; writing—original draft, M.N.R.N., M.F.N.T., and A.A.; writing—review and editing, T.S.B., N.M.K. and M.M. All authors have read and agreed to the published version of the manuscript.

Funding: The authors would like to thank the Universiti Malaysia Perlis and the Ministry of Higher Education (MOHE) Malaysia for providing the facilities and support (Fundamental Research Grant Scheme (FRGS) under grant numbers ofFRGS/1/2019/TK07/UNIMAP/03/1.

Institutional Review Board Statement: Not applicable.

Informed Consent Statement: Not applicable.

Data Availability Statement: Not applicable.

Conflicts of Interest: The authors declare no conflict of interest.

References

1. Vysakh, M.; Azharuddin, M.; Vilas, H.; Muralidhar, K.; Paul, D.; Jacob, B.; Rajasekar, N. Maximum power point tracking using modified PSO with CUK Converter. In Proceedings of the 2014 International Conference on Advances in Electrical Engineering (ICAEE), Singapore, 19 February 2014; pp. 1–6.
2. Manoharan, P.; Subramaniam, U.; Babu, T.S.; Padmanaban, S.; Holm-Nielsen, J.B.; Mitolo, M.; Ravichandran, S. Improved perturb & observation maximum power point tracking technique for solar photovoltaic power generation systems. *IEEE Syst. J.* **2020**, 1–13. [CrossRef]
3. Kumar, N.M.; Yadav, S.K.; Chopra, S.S.; Bajpai, U.; Gupta, R.P.; Padmanaban, S.; Blaabjerg, F. Operational performance of on-grid solar photovoltaic system integrated into pre-fabricated portable cabin buildings in warm and temperate climates. *Energy Sustain. Dev.* **2020**, *57*, 109–118. [CrossRef]
4. Shamshuddin, M.A.; Babu, T.S.; Dragicevic, T.; Miyatake, M.; Rajasekar, N. Priority-based energy management technique for integration of solar PV, battery, and fuel cell systems in an autonomous DC microgrid. *Electr. Power Components Syst.* **2017**, *45*, 1881–1891. [CrossRef]
5. Dalia, Y.; Babu, T.S.; Allam, D.; Ramachandaramurthy, V.; Beshr, E.; Eteiba, M. Fractional chaos maps with flower pollination algorithm for partial shading mitigation of photovoltaic systems. *Energies* **2019**, *12*, 3548.
6. Dalia, Y.; Babu, T.S.; Allam, D.; Ramachandaramurthy, V.K.; Eteiba, M.B. A novel chaotic flower pollination algorithm for global maximum power point tracking for photovoltaic system under partial shading conditions. *IEEE Access* **2019**, *7*, 121432–121445.
7. Malvoni, M.; Kumar, N.M.; Chopra, S.S.; Hatziargyriou, N. Performance and degradation assessment of large-scale grid-connected solar photovoltaic power plant in tropical semi-arid environment of India. *Sol. Energy* **2020**, *203*, 101–113. [CrossRef]
8. Kumar, M.S.; Vishnupriyan, J.; Kumar, N.M. Model Predictive Control Strategy-based Voltage Sensing of Quasi Z-Source Cascaded Multi-Level PV Inverter with Distributed MPPT Algorithm. *Int. J. Renew. Energy Res.* **2020**, *10*, 183–192.
9. Ram, J.P.; Babu, T.S.; Rajasekar, N. Fpa based approach for solar maximum power point tracking. In Proceedings of the 2016 IEEE 6th International Conference on Power Systems (ICPS), New Delhi, India, 4–6 March 2016; pp. 1–6.
10. Femia, N.; Petrone, G.; Spagnuolo, G.; Vitelli, M. Optimization of perturb and observe maximum power point tracking method. *IEEE Trans. Power Electron.* **2005**, *20*, 963–973. [CrossRef]
11. Safari, A.; Mekhilef, S. Simulation and hardware implementation of incremental conductance MPPT with direct control method using cuk converter. *IEEE Trans. Ind. Electron.* **2011**, *58*, 1154–1161. [CrossRef]
12. Tan, C.Y.; Rahim, N.A.; Selvaraj, J. Employing dual scaling mode for adaptive hill climbing method on buck converter. *IET Renew. Power Gener.* **2015**, *9*, 1010–1018. [CrossRef]
13. Babu, G.G.; Sudhakar, T.; Rajasekar, N.; Sangeetha, K. Modified particle swarm optimization technique based maximum power point tracking for uniform and under partial shading condition. *Appl. Soft Comput.* **2015**, *34*, 613–624. [CrossRef]
14. Ajmal, A.M.; Babu, T.S.; Ramachandaramurthy, V.K.; Yousri, D.; Ekanayake, J.B. Static and dynamic reconfiguration approaches for mitigation of partial shading influence in photovoltaic arrays. *Sustain. Energy Technol. Assessments* **2020**, *40*, 100738. [CrossRef]
15. Darussalam, R.; Pramana, R.I.; Rajani, A. Experimental Investigation of Serial Parallel and Total-Cross-Tied Configuration Photovoltaic Under Partial Shading Conditions. In Proceedings of the 2017 International Conference on Sustainable Energy Engineering and Application (ICSEEA), Jakarta, Indonesia, 23–24 October 2017; pp. 140–144.
16. Deshkar, S.N.; Dhale, S.B.; Mukherjee, J.S.; Babu, T.S.; Rajasekar, N. Solar PV array reconfiguration under partial shading conditions for maximum power extraction using genetic algorithm. *Renew. Sustain. Energy Rev.* **2015**, *43*, 102–110. [CrossRef]
17. Rajan, N.A.; Shrikant, K.D.; Dhanalakshmi, B.; Rajasekar, N. Solar PV array reconfiguration using the concept of Standard deviation and Genetic Algorithm. *Energy Procedia* **2017**, *117*, 1062–1069. [CrossRef]
18. Balato, M.; Costanzo, L.; Vitelli, M. Series-Parallel PV array reconfiguration: Maximization of the extraction of energy and much more. *Appl. Energy* **2015**, *159*, 145–160. [CrossRef]
19. Babu, T.S.; Ram, J.P.; Dragicevic, T.; Miyatake, M.; Blaabjerg, F.; Rajasekar, N. Particle Swarm Optimization based Solar PV Array Reconfiguration of the Maximum Power Extraction under Partial Shading Conditions. *IEEE Trans. Sustain. Energy* **2017**, *9*, 74–85. [CrossRef]
20. Tajuddin, M.F.N.; Arif, M.S.; Ayob, S.M.; Salam, Z. Perturbative methods for maximum power point tracking (MPPT) of photovoltaic (PV) systems: A review. *Int. J. Energy Res.* **2015**, *39*, 1153–1178. [CrossRef]
21. Ishaque, K.; Salam, Z. A Deterministic Particle Swarm Optimization Maximum Power Point Tracker for Photovoltaic System under Partial Shading Condition. *IEEE Trans. Ind. Electron.* **2012**, *60*, 1. [CrossRef]

22. Rani, B.I.; Ilango, G.S.; Nagamani, C. Enhanced power generation from PV array under partial shading conditions by shade dispersion using Su Do Ku configuration. *IEEE Trans. Sustain. Energy* **2013**, *4*, 594–601. [CrossRef]
23. IIyer, S.R. Performance Comparison of Zig-Zag and Su Do Ku Schemes in a Partially Shaded Photo Voltaic Array under Static Shadow Conditions. In Proceedings of the 2017 Innovations in Power and Advanced Computing Technologies (i-PACT), Vellore, India, 21–22 April 2017; pp. 17–22.
24. Rao, P.S.; Ilango, G.S.; Nagamani, C. Maximum power from PV arrays using a fixed configuration under different shading conditions. *IEEE J. Photovoltaics* **2014**, *4*, 679–686. [CrossRef]
25. Yousri, D.; Babu, T.S.; Mirjalili, S.; Rajasekar, N.; Elaziz, M.A. A novel objective function with artificial ecosystem-based optimization for relieving the mismatching power loss of large-scale photovoltaic array. *Energy Convers. Manag.* **2020**, *225*, 113385. [CrossRef]
26. Liu, Y.; Pang, Z.; Cheng, Z. Research on an adaptive solar photovoltaic array using shading degree model-based reconfiguration algorithm. In Proceedings of the 2010 Chinese Control and Decision Conference, Xuzhou, China, 26–28 May 2010; pp. 2356–2360. [CrossRef]
27. Yousri, D.; Thanikanti, S.B.; Balasubramanian, K.; Osama, A.; Fathy, A. Multi-Objective Grey Wolf Optimizer for Optimal Design of Switching Matrix for Shaded PV array Dynamic Reconfiguration. *IEEE Access* **2020**, *8*, 159931–159946. [CrossRef]
28. Wohlgemuth, J.; Herrmann, W. Hot spot tests for crystalline silicon modules. In Proceedings of the 31st IEEE Photovoltaic Specialists Conference, Lake Buena Vista, FL, USA, 3–7 January 2005; pp. 1062–1065.
29. Rajput, P.; Tiwari, G.; Sastry, O. Thermal modelling and experimental validation of hot spot in crystalline silicon photovoltaic modules for real outdoor condition. *Sol. Energy* **2016**, *139*, 569–580. [CrossRef]
30. Babu, T.S.; Yousri, D.; Balasubramanian, K. Photovoltaic array reconfiguration system for maximizing the harvested power using population-based algorithms. *IEEE Access* **2020**, *8*, 109608–109624. [CrossRef]
31. Yousri, D.; Babu, T.S.; Beshr, E.; Eteiba, M.B.; Allam, D. A robust strategy based on marine predators algorithm for large scale photovoltaic array reconfiguration to mitigate the partial shading effect on the performance of PV system. *IEEE Access* **2020**, *8*, 112407–112426. [CrossRef]
32. Parlak, K.Ş. PV array reconfiguration method under partial shading conditions. *Int. J. Electr. Power Energy Syst.* **2014**, *63*, 713–721. [CrossRef]
33. Horoufiany, M.; Ghandehari, R. Optimization of the Sudoku based reconfiguration technique for PV arrays power enhancement under mutual shading conditions. *Sol. Energy* **2018**, *159*, 1037–1046. [CrossRef]
34. Chao, K.-H.; Lai, P.-L.; Liao, B.-J. The optimal configuration of photovoltaic module arrays based on adaptive switching controls. *Energy Convers. Manag.* **2015**, *100*, 157–167. [CrossRef]
35. Nguyen, D.; Lehman, B. An adaptive solar photovoltaic array using model-based reconfiguration algorithm. *IEEE Trans. Ind. Electron.* **2008**, *55*, 2644–2654. [CrossRef]
36. Jazayeri, M.; Jazayeri, K.; Uysal, S. Adaptive photovoltaic array reconfiguration based on real cloud patterns to mitigate effects of non-uniform spatial irradiance profiles. *Sol. Energy* **2017**, *155*, 506–516. [CrossRef]
37. Velasco-Quesada, G.; Guinjoan-Gispert, F.; Pique-Lopez, R.; Roman-Lumbreras, M.; Conesa-Roca, A. Electrical PV array reconfiguration strategy for energy extraction improvement in grid-connected PV systems. *IEEE Trans. Ind. Electron.* **2009**, *56*, 4319–4331. [CrossRef]
38. Balato, M.; Costanzo, L.; Vitelli, M. Series-parallel PV arrays: A comparison between the performances of two algorithms for strings with an equal or with a different number of PV modules. In Proceedings of the 2016 IEEE International Power Electronics and Motion Control Conference, PEMC, Varna, Bulgaria, 25–28 September 2016; pp. 1269–1274. [CrossRef]
39. La Manna, D.; Vigni, V.L.; Sanseverino, E.R.; Di Dio, V.; Romano, P. Reconfigurable electrical interconnection strategies for photovoltaic arrays: A review. *Renew. Sustain. Energy Rev.* **2014**, *33*, 412–426. [CrossRef]
40. Rao, P.S.; Dinesh, P.; Ilango, G.S.; Nagamani, C. Optimal Su-Do-Ku based interconnection scheme for increased power output from PV array under partial shading conditions. *Front. Energy* **2015**, *9*, 199–210. [CrossRef]
41. Villalva, M.G.; Gazoli, J.R.; Filho, E.R. Comprehensive Approach to Modeling and Simulation of Photovoltaic Arrays. *IEEE Trans. Power Electron.* **2009**, *24*, 1198–1208. [CrossRef]
42. De Soto, W.; Klein, S.; Beckman, W. Improvement and validation of a model for photovoltaic array performance. *Sol. Energy* **2006**, *80*, 78–88. [CrossRef]
43. Sera, D.; Teodorescu, R.; Rodriguez, P. PV panel model based on datasheet values. In Proceedings of the IEEE International Symposium on Industrial Electronics, Vigo, Spain, 4-7 June 2007; pp. 2392–2396. [CrossRef]
44. Yadir, S.; Benhmida, M.; Sidki, M.; Assaid, E.; Khaidar, M. New method for extracting the model physical parameters of solar cells using explicit analytic solutions of current-voltage equation. In Proceedings of the 2009 International Conference on Microelectronics (ICM 2009), Marrakech, Morocco, 19–22 December 2009; pp. 390–393. [CrossRef]
45. Patnaik, B.; Mohod, J.D.; Duttagupta, S.P. Distributed multi-sensor network for real time monitoring of illumination states for a reconfigurable solar photovoltaic array. In Proceedings of the ISPTS-1, 1st International Symposium on Physics and Technology of Sensors, Pune, India, 7–10 March 2012; pp. 106–109. [CrossRef]
46. Aydilek, İ.B. A Hybrid Firefly and Particle Swarm Optimization Algorithm for Computationally Expensive Numerical Problems. *Appl. Soft Comput.* **2018**, *66*, 232–249. [CrossRef]

47. Chiewchanchairat, K.; Bumroongsri, P.; Kheawhom, S. Reconfiguration of distribution system with distributed generation using Firefly algorithm. *KKU Eng. J.* **2015**, *42*, 107–115. [CrossRef]
48. Tze, C.; Kho, K.; Ahmed, J.; Kashem, S.; Lung, Y. A comprehensive review on PV configurations to maximize power under partial shading. In Proceedings of the TENCON 2017-2017 IEEE Region 10 Conference, Penang, Malaysia, 5–8 November 2017; pp. 763–768. [CrossRef]
49. Wu, Z.; Zhang, C.; Alkahtani, M.; Hu, Y.; Zhang, J. Cost Effective Offline Reconfiguration for Large-Scale Non-Uniformly Aging Photovoltaic Arrays Efficiency Enhancement. *IEEE Access* **2020**, *8*, 80572–80581. [CrossRef]